Bioconjugate Chemistry

Article

pubs.acs.org/bc

Synthesis and Biological Properties of Quilamines II, New Iron Chelators with Antiproliferative Activities

Vincent Corcé,[†,‡,§] Stéphanie Renaud,[‡,§] Isabelle Cannie,[‡,§] Karine Julienne,[†] Sébastien G. Gouin,[†] Olivier Loréal,[‡,§] François Gaboriau,*[,‡,§] and David Deniaud*[,†]

[†]LUNAM Université, CEISAM, Chimie Et Interdisciplinarité, Synthèse, Analyse, Modélisation, UMR CNRS 6230, UFR des Sciences et des Techniques, 2, rue de la Houssinière, BP 92208, 44322 Nantes Cedex 3, France

[‡]INSERM, UMR 991, CHRU Pontchaillou, 35033 Rennes, France

[§]Université de Rennes 1, 35043 Rennes, France

ABSTRACT: To selectively target tumor cells expressing an overactive Polyamine Transport System (PTS), we designed, synthesized, and evaluated the biological activity of a new generation of iron chelators, derived from the lead compound **HQ1−44**, which we named Quilamines II. The structures of four new antiproliferative agents were developed. They differ in the size of the linker (**HQ0−44** and **HQ2−44**) or in the nature of the linker (**HQCO-44** and **HQCS-44**) between a hydroxyquinoline moiety (HQ) and a homospermidine (44) chain, the best polyamine vector. The Quilamines II were obtained after 6 to 9 steps by Michael addition, peptide linkage, and reductive amination or by using the Willgerodt-Kindler reaction. The biological evaluation of these second-generation Quilamines showed that modifying the size of the linker increased the selectivity of these compounds for the PTS. In addition, measurement of the toxicity of Quilamines **HQ0−44** and **HQ2−44** highlighted their marked antiproliferative nature on several cancerous cell lines as well as a differential activity on nontransformed cells (fibroblasts). In contrast, Quilamines **HQCO-44** and **HQCS-44** presented low selectivity for the PTS, probably due to a loss of electrostatic interaction. We also demonstrated that the HCT116 cell line, originating from a human colon adenocarcinoma, was the most responsive to the various Quilamines. As deduced from the calcein and HVA assays, the higher iron chelating capacity of **HQ1−44** could explain its higher antiproliferative efficiency.

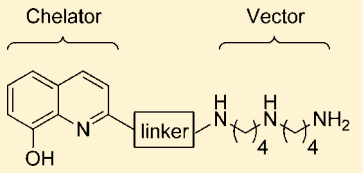

linker: C=O, C=S, $(CH_2)_x$; x = 0, 1 or 2

Quilamines II

INTRODUCTION

Iron is a cofactor of various enzymes and thus plays a key role in biological processes including energy generation by oxidative phosphorylation[1] and cell growth and proliferation by regulating the activity of ribonucleotide reductase (RR) involved in DNA synthesis.[2,3] In tumoral cells, the DNA synthesis rate is higher than in healthy cells and it has been shown that both the activity and the expression of RR increase during tumor growth.[4]

There are a number of alterations in iron metabolism in tumor cells leading to increased iron ingress via the transferrin receptor (TfR1) and to decreased iron egress by ferroportin.[5] In most cancerous cells, the expression of the transferrin 1 receptor (TfR1) is higher than in healthy cells and is proportional to the stage of progress of the tumor.[6,7] Recent studies have shown that levels of ferroportin and hepcidin are disrupted in cancerous cells leading to an accumulation of iron.[8] In breast cancer cells, the expression of ferroportin is reduced, or even absent, at the gene and protein level and is accompanied by a simultaneous increase in the expression of hepcidin.[8,9] Moreover, this drop in ferroportin is associated with a concomitant rise in the labile iron pool (LIP) and a reduction in the level of ferritin. This enhanced requirement for iron by growing tumor cells provides a new research route for iron ligands with antiproliferative effects.[5]

Polyamine metabolism (biosynthesis and uptake), detrimental to cell proliferation, is also particularly amplified in tumor cells.[10] The Polyamine Transport System (PTS), which can deal with natural and synthetic polyamines, is increased in tumor cells.[11] This property is of potential interest for targeting antitumor agents.[12−21] This concept of tumor vectorization by polyamines has also been developed to inhibit their own transporter,[22,23] to vectorize cytotoxic compounds such as dimethylsilane polyamine derivatives[24] or molecules carrying boron atoms for boronotherapy,[25,26] and to monitor the intracellular traffic of polyamines toward cells by using fluorescent polyamine analogues.[18,27−29] More recently, F14512, a novel spermine conjugate associated with etoposide (epipodophyllotoxin), an inhibitor of DNA-topoisomerase II,[30] was selected for clinical development in AML phase I.

Even though neoplastic cells require more iron than normal cells, it seems possible to use a method targeting the chelator selectively toward the tumor cells. To target tumor cells expressing an overactive PTS compared to normal cells, we designed and synthesized a new generation of iron chelators, which we named Quilamines, based on an 8-hydroxyquinoline (8-HQ) scaffold linked to linear polyamine vectors.[31] A set of

Received: October 14, 2013
Revised: January 14, 2014
Published: January 14, 2014

dx.doi.org/10.1021/bc4004734 | *Bioconjugate Chem.* 2014, 25, 320−334

Quilamines bearing variable polyamine chains was designed and assessed for their ability to interact with iron. Quilamines were also screened for their cytostatic/cytotoxic effects and their selective uptake by the PTS in the CHO cell line. **HQ1−44**, the most promising Quilamine identified, contains a homospermidine moiety and was shown to display an efficient antiproliferative activity in the micromolar range. The homospermidine cargo (44) was shown to be the most selectively transported by the PTS and to be involved in iron coordination. We also demonstrated the high complexation capacity of **HQ1−44** with iron, while much weaker complexes were formed with other cations, indicative of a high selectivity. The **HQ1−44** ligand utilizes an O,N,N-donor set and, in view of the stoichiometry, it could be assumed that the iron complex [Fe/**HQ1−44**] forms three five-membered chelate rings. In fact, the ferric complex adopted a 1:2 stoichiometry at pH = 7.4 in which the iron was probably coordinated by two vicinal N-atoms and a hydroxyl group (Figure 1).

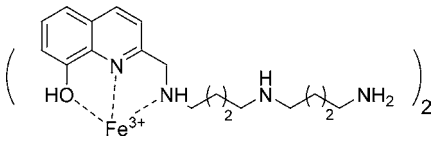

Figure 1. Hypothetical structure of the **HQ1−44**/Fe complex.

In terms of chemistry, we would like to improve the iron-chelating efficiency in order to increase the antiproliferative activity of **HQ1−44** by modifying the length and the nature of the spacer between the chelating moiety and the homospermidine chain.

Our objective was to develop new polyaminoquinoline iron chelators, derived from the lead **HQ1−44**, which we named Quilamines II. The structures of the four new antiproliferative agents developed differ in the size of the linker (**HQ0−44** and **HQ2−44**) or in the nature of the linker (**HQCO-44** and **HQCS-44**) between a hydroxyquinoline moiety (HQ) and a homospermidine (44) chain, the best vector. For **HQ0−44** and **HQ2−44**, the introduction of zero or two carbon atoms will probably have a significant effect on the stability of the iron complexes formed by modification of the size of the chelate rings (Figure 2, top). Ligands **HQCO-44** and **HQCS-44** differ only in the nature of their heteroatom, which is either oxygen or sulfur. As these ligands contain amide or thioamide functions, the iron would be chelated by nitrogen, oxygen, or sulfur atoms by simple rotation (Figure 2, bottom). Our hypothesis was that, depending on the "hard/soft" nature of the heteroatom, the ligands should lead to notable differences in complexation, and thus change the antiproliferative activity.

EXPERIMENTAL SECTION

Chemistry. NMR spectra were recorded at room temperature with a Bruker Avance 300 Ultra Shield or a Bruker Avance III 400 spectrometer. Chemical shifts are reported in parts per million (ppm); coupling constants are reported in units of Hertz [Hz]. Infrared (IR) spectra were recorded with a Bruker Vector 22 FTIR using KBr films or KBr pellets. Low-resolution mass spectra (MS) were recorded with a Thermo Electron DSQ spectrometer. High-resolution mass spectra (HRMS) were recorded with a Thermo Fisher Hybrid LTQ-orbitrap spectrometer (ESI^+) and a Bruker Autoflex III SmartBeam spectrometer (MALDI). Microanalyses were performed on a Thermo Scientific FLASH 2000 Series CHNS/O Analyzer. Melting points were determined in open capillary tubes and are uncorrected. All reagents were purchased from Acros Organics or Aldrich and were used without further purification. Column chromatographs were conducted on silica gel Kieselgel SI60 (40−63 μm) from Merck. Reactions requiring anhydrous conditions were performed under argon. Dichloromethane, acetonitrile, and MeOH were distilled over CaH_2, THF over Na/benzophenone. Dichloroethane, DMSO, and DMF were used dry from secure sealed bottles.

Compounds **1**, **3−5**, **13**, and **14** have already been described in the literature.

2-(2-oxoethyl)quinolin-8-yl Acetate (2). Oxalyl chloride (1.2 equiv, 0.36 mmol) in dichloromethane (3 mL) was added to a solution of dimethylsulfoxide (2.4 equiv, 0.72 mmol) in dichloromethane (150 μL), and the mixture was stirred at −78 °C for 30 min under Ar. Alcohol **7** (1 equiv, 0.3 mmol) in dichloromethane (1 mL) was added dropwise, and the resulting mixture was then stirred for 30 min at −78 °C. Triethylamine (4.8 equiv, 1.44 mmol) was added dropwise, and the resulting mixture was then stirred for 15 min at −78 °C; then, the

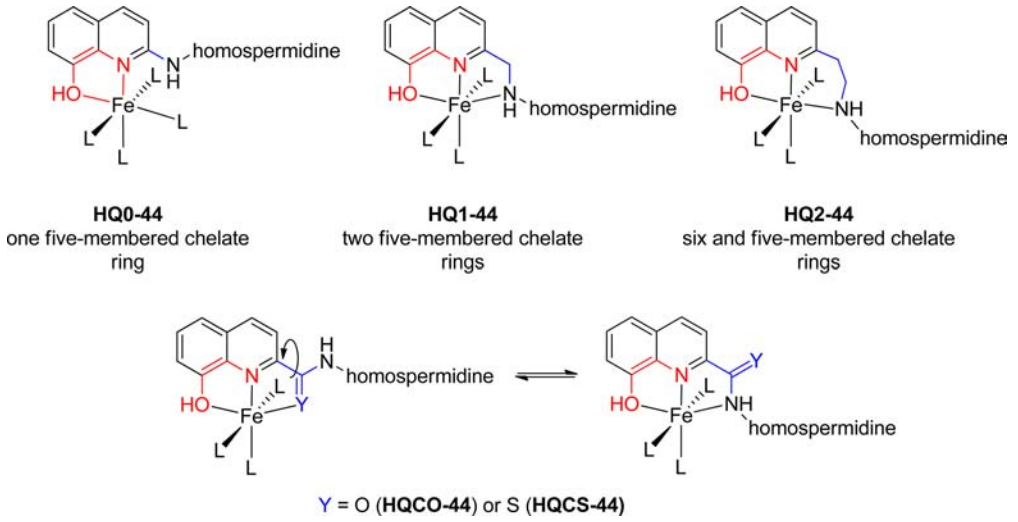

Figure 2. Hypothetical structures of iron complexes with different sizes of chelate rings or different heteroatoms.

dx.doi.org/10.1021/bc4004734 | *Bioconjugate Chem.* 2014, 25, 320−334

temperature was increased to room temperature over a period of 1 h. The mixture was quenched by addition of water (4 mL) and extracted with CH_2Cl_2. The organic extracts were dried over Na_2SO_4, filtered, and concentrated under reduced pressure and the residue was purified by chromatography on silica gel (CH_2Cl_2/EtOAc (9:1)) to give compound **2** as a red solid (75%). ^{1}H NMR ($CDCl_3$, 300 MHz): δ = 2.59 (s, 3H, CH_3), 5.41 (d, 1H, ^3J = 3.6 Hz, *H*), 6.81 and 7.69 (system AB, 2H, ^3J = 9 Hz, H^3 and H^4), 7.27 (m, 1H), 7.23−7.47 (m, 3H), 8.75 (s-e, 1H, *H*), 15.21 (s-e, 1H, O*H*) ppm. ^{13}C NMR ($CDCl_3$, 75 MHz): δ = 21.1 (*C*H$_3$), 95.1, 121.8, 123.4, 124.6, 124.8, 131.2, 136.3, 139.2, 153.6, 169.0, 179.9 (*C*═O) ppm. HRMS (MALDI): calcd. for $C_{13}H_{12}NO_3$ $[M+H]^+$ 229.2313; found 229.2351.

*2-(2-Hydroxyethyl)quinolin-8-ol (**6**).* *n*-Butyllithium (2.2 equiv, 13.86 mmol) was added dropwise to a stirring solution of 8-hydroxyquinaldine (1 equiv, 6.3 mmol) in tetrahydrofuran (20 mL) at −78 °C for 1 h under Ar. Paraformaldehyde (4 equiv, 50.4 mmol) was added at −78 °C, and the temperature was increased to room temperature over a period of 1 h. The mixture was quenched by addition of sodium hydrogen carbonate (20 mL) at −78 °C and extracted with diethylether. The organic extracts were dried over Na_2SO_4, filtered, and concentrated under reduced pressure and the residue was purified by chromatography on silica gel (CH_2Cl_2/MeOH (9.6:0.4)) to give compound **6** as a white solid (88%). IR (KBr): γ = 3156, 3086, 2950, 1565, 1436, 1383, 1322, 1269, 1088, 1055, 1036, 820 cm^{-1}. ^{1}H NMR ($CDCl_3$, 400 MHz): δ = 3.20 (t, 2H, ^3J = 6.2 Hz, CH_2), 4.14 (t, 2H, ^3J = 6.2 Hz, CH_2), 7.16 (dd, 1H, ^3J = 8 Hz, ^4J = 3.2 Hz, H^7_{ar}), 7.28 (dd, 1H, ^3J = 8 Hz, ^4J = 3.2 Hz, H^5_{ar}), 7.34 and 8.08 (system AB, 2H, ^3J = 8.4 Hz, H^3_{ar} and H^4_{ar}), 7.39 (t, 2H, ^3J = 8 Hz, H^6_{ar}) ppm. ^{13}C NMR ($CDCl_3$, 100 MHz): δ = 40.7 (*C*H$_2$), 61.5 *C*H$_2$), 110.6 (*C*^{7}), 117.9 (*C*^{5}), 122.8 (*C*^{3}), 127.2 (*C*^{8a}), 127.3 (*C*^{6}), 136.8 (*C*^{4}), 137.7 (*C*^{4a}), 151.7 (*C*^{2}) 158.1 (*C*^{8}) ppm. HRMS (ESI+): calcd. for $C_{11}H_{12}NO_2$ $[M+H]^+$ 190.08680; found 190.08614.

*2-(2-Hydroxyethyl)quinolin-8-yl acetate (**7**).* A solution of sodium hydroxide 1 M (30 mL) and acetic anhydride (2 equiv, 5.28 mmol) was added to a solution of compound **6** (1 equiv, 2.64 mmol) in dichloromethane (30 mL), and the mixture was stirred at r.t. for 3 h. The mixture was extracted with dichloromethane, dried over Na_2SO_4, filtered, and concentrated under reduced pressure and the residue was purified by chromatography on silica gel (CH_2Cl_2/EtOAc: (9:1)) to give compound 7 as a yellow solid (90%). ^{1}H NMR ($CDCl_3$, 300 MHz): δ = 2.50 (s, 3H, CH_3), 3.20 (t, 2H, ^3J = 6.2 Hz, CH_2), 4.14 (t, 2H, ^3J = 6.2 Hz, CH_2), 7.31 and 8.13 (system AB, 2H, ^3J = 8.4 Hz, H^3_{ar} and H^4_{ar}), 7.44 (dd, 1H, ^3J = 9 Hz, ^4J = 3 Hz, H^5_{ar}), 7.51 (t, 2H, ^3J = 8 Hz, H^6_{ar}), 7.70 (dd, 1H, ^3J = 9 Hz, ^4J = 3 Hz, H^7_{ar}) ppm. ^{13}C NMR ($CDCl_3$, 75 MHz,): δ = 20.9 (*C*H$_3$), 38.9 (*C*H$_2$), 61.0 (*C*H$_2$), 121.9 (*C*^{5}), 122.7 (*C*^{3}), 125.8 (*C*^{7}), 126.0 (*C*^{6}), 128.1 (*C*^{8a}), 136.9 (*C*^{4}), 139.8 (*C*^{4a}), 146.7 (*C*^{2}), 161.6 (*C*^{8}), 169.9 (C═O) ppm. HRMS (ESI+): calcd. for $C_{13}H_{14}NO_3$ $[M+H]^+$ 232.09737; found 232.09769.

*2-Vinylquinolin-8-ol (**8**).* Triethylamine (5 equiv, 15.85 mmol) and methanesulfonyl chloride (3 equiv, 9.51 mmol) were added to a solution of compound **6** (1 equiv, 3.17 mmol) in dichloromethane (30 mL) at 0 °C and the mixture was stirred at r.t. for 3 h. Solvent was evaporated, the resulting solid was solubilized in the minimum of EtOH, and an aqueous solution of sodium hydroxide (1 M, 30 mL) was added. The mixture was stirred for 5 h at reflux and then neutralized with HCl 1 M to pH = 7. The solution was extracted with dichloromethane, dried over Na_2SO_4, filtered, and concentrated under reduced pressure and the residue was purified by chromatography on silica gel (CH_2Cl_2) to give compound **8** as a white solid (96%). IR (KBr): γ = 3064, 1614, 1561, 1514, 1436, 1377, 1339, 1293, 1243, 1091, 984 cm^{-1}. ^{1}H NMR ($CDCl_3$, 400 MHz): δ = 5.64 (dd, 1H, ^3J = 10.85 Hz, ^2J = 0.9 Hz, CH_2), 6.31 (dd, 1H, ^3J = 17.7 Hz, ^2J = 0.9 Hz, CH_2), 6.99 (dd, 1H, ^3J = 17.7 Hz, ^3J = 10.85 Hz, C*H*), 7.16 (dd, 1H, ^3J = 7.64 Hz, ^4J = 1.2 Hz, H^7_{ar}), 7.28 (dd, 1H, ^3J = 8.25 Hz, ^4J = 1.2 Hz, H^5_{ar}), 7.40 (dd, 1H, ^3J = 7.64 Hz, ^3J = 8.25 Hz, H^6_{ar}), 7.57 and 8.09 (system AB, 2H, ^3J = 8.4 Hz, H^3_{ar} and H^4_{ar}) ppm. ^{13}C NMR ($CDCl_3$, 100 MHz): δ = 110.2 (*C*^{7}), 117.7 (*C*^{5}), 119.5 (*C*^{3}), 119.8 (*C*H$_2$), 127.6 (*C*^{4a}), 127.8 (*C*^{6}), 136.5 (*C*^{4}), 137.3 (*C*H), 137.9 (*C*^{8a}), 152.3 (*C*^{8}), 153.8 (*C*^{2}) ppm. HRMS (ESI +): calcd. for $C_{11}H_{10}NO$ $[M+H]^+$; 172.07569; found 172.07562. Anal. Calcd. for $C_{11}H_9NO$: C, 77.17; H, 5.30; N, 8.18. Found: C, 77.10; H, 5.41; N, 8.09.

*2-[4-tert-Butyloxycarbonyl-(4-N-tert-butyloxycarbonyl-aminobutyl)aminobutyl]amino ethylquinolin-8-ol (**9**).* 2-Vinylquinolin-8-ol (**8**) (1 equiv, 0.52 mmol) was added to a stirring solution of amine **1** (1 equiv, 0.52 mmol) in methanol (5 mL), and then 3 drops of acetic acid were added and the mixture was stirred at 70 °C for 24 h. It was then concentrated under reduced pressure, dichloromethane was added, and the mixture was washed with saturated aqueous $NaHCO_3$ and water. The organic extracts were dried over Na_2SO_4, filtered, and concentrated under reduced pressure; and the residue was purified by chromatography on silica gel (CH_3Cl/MeOH/NH_4OH: (8.5:0.4:0.1)) to give compound **9** as a yellow oil (64%). IR (KBr): γ = 3383, 1668, 1455, 1390, 1251, 1089, 869 cm^{-1}. ^{1}H NMR (CD_3OD, 400 MHz): δ = 1.37−1.65 (m, 26H, 2 CH_2CH_2 and 3 C(CH_3)$_3$), 2.82 (br s, 2H), 3.03 (t, 2H, ^3J = 6.8 Hz, BocNHCH_2), 3.12−3.29 (m, 8H), 7.09 (dd, 1H, ^3J = 7.4 Hz, ^4J = 1.5 Hz, H^7_{ar}), 7.32 (dd, 1H, ^3J = 8.25 Hz, ^4J = 1.5 Hz, H^5_{ar}), 7.35−7.44 (m, 2H, H^3_{ar} and H^6_{ar}), 8.18 (d, 1H, ^3J = 8.25 Hz, H^4_{ar}) ppm. ^{13}C NMR (CD_3OD, 100 MHz): δ = 26.9 (3 CH$_2$), 28.3 (CH$_2$), 28.7 (C(CH$_3$)$_3$), 28.8 (C(CH$_3$)$_3$), 36.9 (CH$_2$), 40.9 (CH$_2$), 48.1 (3 CH$_2$), 49.0 (CH$_2$), 79.8 (C(CH$_3$)$_3$), 80.9 (C(CH$_3$)$_3$), 112.3 (*C*^{7}), 118.9 (*C*^{5}), 123.2 (*C*^{3}), 128.1 (*C*^{4a}), 129.1 (*C*^{6}), 138.1 (*C*^{8a}), 139.4 (*C*^{4}), 153.9 (*C*^{2}), 157.4 (*C*^{8}), 158,5 (C═O) ; 159,2 (C═O) ppm. HRMS (MALDI): calcd. for $C_{29}H_{47}N_4O_5$ $[M+H]^+$; 531.3541; found 531.3544.

*4-tert-Butyloxycarbonyl-(4-tert-butyloxycarbonyl-aminobutyl)aminobutanal (**10**).* Bis acetoxyiodobenzene (1.1 equiv, 1.1 mmol) and 2,2,6,6-tetramethylpiperidine-1-oxyl (0.1 equiv, 0.1 mmol) were added to a stirring solution of aminoalcohol **14** (1 equiv, 1 mmol) in dichloromethane (1 mL) at r.t. for 5 h under Ar. Dichloromethane was added and the organic solution was washed with saturated aqueous $Na_2S_2O_3$, $NaHCO_3$, brine, and water. The organic extracts were dried over Na_2SO_4, filtered, and concentrated under reduced pressure; and the residue was purified by chromatography on silica gel (CH_2Cl_2/EtOAc: (8:2)) to give compound **9** as a colorless oil (75%). IR (film): γ = 2974, 2930, 2867, 1694, 1479, 1390, 1168 cm^{-1}. ^{1}H NMR ($CDCl_3$, 400 MHz): δ = 1.35−1.62 (m, 22H, CH_2CH_2 and 2 C(CH_3)$_3$), 1.83 (qt, 2H, ^3J = 7.1 Hz, CH_2^3), 2.44 (t, 2H, ^3J = 7.1 Hz, CH_2^2), 3.04−3.27 (m, 6H), 4.56 (br s, 1H, N*H*), 9.77 (s, 1H, C*H*O) ppm. ^{13}C NMR ($CDCl_3$, 100 MHz): δ = 21.2 (CH$_2$), 25.8 (CH$_2$), 27.6 (CH$_2$), 28.5 (C(CH$_3$)$_3$), 28.6 (C(CH$_3$)$_3$), 40.3 (CH$_2$), 41.2 (CH$_2$),46.3 (CH$_2$), 46.8 (CH$_2$), 79.3 (C(CH$_3$)$_3$), 79.7 (C(CH$_3$)$_3$), 155.7 (C═O), 156.1 (C═O), 201.7 (CHO)

dx.doi.org/10.1021/bc4004734 | *Bioconjugate Chem.* 2014, 25, 320−334

ppm. HRMS (MALDI): calcd. for $C_{18}H_{34}NaN_2O_5$ $[M+Na]^+$; 381.2360; found 381.2366.

*4-(4-Hydroxybutyl)aminobutanenitrile (**11**).* Potassium carbonate (1.5 equiv, 15 mmol) and 4-bromobutanenitrile (1 equiv, 10 mmol) were added to a stirring solution of 4-aminobutanol (1 equiv, 10 mmol) in acetonitrile (100 mL) at 50 °C for 16 h under Ar. After filtration, the solvent was removed under reduced pressure and the residue was purified by chromatography on silica gel (CH_3Cl/MeOH/NH_4OH (8.9:1.0:0.1)) to give compound **11** as a colorless oil (56%). IR (film): γ = 3357, 2936, 2865, 1694, 1652, 1542, 1375, 1249, 1059 cm^{-1}. ^1H NMR ($CDCl_3$, 300 MHz): δ = 1.57−1.69 (m, 4H, CH_2CH_2), 1.84 (qt, 2H, ^3J = 7.1 Hz, CH_2^3), 2.44 (t, 2H, ^3J = 7.2 Hz, CH_2^2), 2.66 (t, 2H, ^3J = 5.4 Hz, CH_2NH), 2.76 (t, 2H, ^3J = 6.9 Hz, CH_2^4), 3.57 (t, 2H, ^3J = 5.1 Hz, CH_2OH) ppm. ^{13}C NMR ($CDCl_3$, 75 MHz): δ = 15.2 (CH_2^2), 25.6 (CH_2^3), 28.4 and 32.3 (CH_2CH_2), 47.9 (CH_2^4), 49.8 (CH_2NH), 62.7 (CH_2OH), 119.5 (CN) ppm. HRMS (ESI+): calcd. for $C_8H_{17}N_2O$ $[M+H]^+$; 157.13354; found 157.13348.

*4-tert-Butyloxycarbonyl-(4-hydroxybutyl)amino-butanenitrile (**12**).* A solution of di-*tert*-butyldicarbonate (1.5 equiv, 1.34 mmol) was added to a stirring solution of **11** (1 equiv, 0.896 mmol) in a solution of methanol and 10% triethylamine (10 mL). After stirring for 24 h at room temperature, solvents were removed under reduced pressure to give a colorless oil which was dissolved in dichloromethane, washed with saturated $NaHCO_3$ and water, dried over Na_2SO_4, filtered, and concentrated under reduced pressure. The residue was purified by chromatography on silica gel (CH_2Cl_2/EtOAc (6:4)) to give compound **12** as a colorless oil. IR (film): γ = 3442, 2974, 2931, 1685, 1479, 1420, 1296, 1167, 1057 cm^{-1}. ^1H NMR ($CDCl_3$, 300 MHz): δ = 1.45 (s, 9H, $C(CH_3)_3$), 1.49−1.66 (m, 4H, CH_2CH_2), 1.89 (qt, 2H, ^3J = 7.1 Hz, CH_2^3), 2.35 (t, 2H, ^3J = 7.1 Hz, CH_2^2), 3.22 (br t, 2H, CH_2NBoc), 3.31 (t, 2H, ^3J = 6.9 Hz, CH_2^4), 3.66 (t, 2H, ^3J = 6 Hz, CH_2OH) ppm. ^{13}C NMR ($CDCl_3$, 75 MHz): δ = 14.9 (CH_2^2), 24.7 (2 CH_2), 28.5 ($C(CH_3)_3$), 29.8 (CH_2), 45.9 (CH_2^4), 47.5 (CH_2NBoc), 62.6 (CH_2OH), 80.2 ($C(CH_3)_3$), 119.5 (CN), 155.7 (C═O) ppm. HRMS (MALDI): calcd. for $_{13}H_{24}NaN_2O_3$ $[M+Na]^+$; 279.1679; found 279.1690.

*2-[4-tert-Butyloxycarbonyl-(4-tert-butyloxycarbonyl-aminobutyl)aminobutyl]aminoquinolin-8-ol (**15**).* To a stirred solution of polyamine **10** (1 equiv, 0.555 mmol) in 1,2-dichloroethane (5 mL) at room temperature under argon was added 2-aminoquinolin-8-ol (1.2 equiv, 0.66 mmol). After 15 min, sodium triacetoxyborohydride (3 equiv, 1.65 mmol) was added and the mixture was stirred for 12 h. The reaction mixture was quenched by adding 1 M NaOH (5 mL), stirred for 30 min; the product was extracted with dichloromethane, dried over Na_2SO_4, filtered, and concentrated under reduced pressure; and the residue was purified by chromatography on silica gel (CH_2Cl_2/EtOAc (8:2)) to give compound **12** as a yellow oil (73%). IR (film): γ = 3366, 2974, 2930, 1683, 1615, 1478, 1391, 1249, 1169 cm^{-1}. ^1H NMR (CD_3OD, 400 MHz): δ = 1.32−1.55 (m, 22H, CH_2CH_2 and 2 $C(CH_3)_3$), 1.59−1.72 (m, 4H, CH_2CH_2), 2.99 (t, 2H, ^3J = 6.7 Hz, $BocNHCH_2$), 3.15 (t, 2H, ^3J = 7.3 Hz), 3.24 (br t, 2H), 3.53 (br t, 2H, $NHCH_2$), 6.72 (d, 1H, ^3J = 8.9 Hz, H^3_{ar}), 6.91 (dd, 1H, ^3J = 7.5 Hz and ^4J = 1.3 Hz, H^7_{ar}), 7.00 (t, 1H, ^3J = 7.7 Hz, H^6_{ar}), 7.06 (dd, 1H, ^3J = 8 Hz and ^4J = 1.3 Hz, H^5_{ar}), 7.75 (d, 1H, ^3J = 8.9 Hz, H^4_{ar}) ppm. ^{13}C NMR (CD_3OD, 100 MHz): δ = 26.9 (2 CH_2), 27.7 (CH_2), 28.3 (CH_2), 28.7 ($C(CH_3)_3$), 28.8 ($C(CH_3)_3$), 40.9 ($BocNHCH_2$), 41.6 (CH_2), 47.9 (2 CH_2), 79.8 ($C(CH_3)_3$), 80.8 ($C(CH_3)_3$), 111.2 (C^7), 114.3 (C^5), 118.8 (C^3), 122.7 (C^{4a}), 124.3 (C^6), 137.7 (C^{8a}), 138.6 (C^4), 151.3 (C^2), 157.5 (C^8), 157.7 (C═O), 158.5 (C═O) ppm. HRMS (MALDI): calcd. for $C_{27}H_{43}N_4O_5$ $[M+H]^+$; 503.3228; found 503.3228.

*N-[4-tert-Butyloxycarbonyl-(4-tert-butyloxycarbonyl-aminobutyl)aminobutyl]-8-hydroxyquinolin-2-carboxamide (**16**).* To a stirred solution of 8-hydroxyquinaldinic acid (1 equiv, 0.94 mmol) in dichloromethane (5 mL) at room temperature under argon was added *N,N′*-dicyclohexylcarbodiimide (1.1 equiv, 1.034 mmol). After 20 min, hydroxybenzotriazole (1.1 equiv, 1.034 mmol) was added and the mixture was stirred at r.t. for 2 h under argon. Then, a solution of amine **1** (1 equiv, 0.94 mmol) was added in dichloromethane (3 mL) at room temperature under argon and the mixture was stirred for 18 h. The mixture was filtered, concentrated under reduced pressure, and the residue purified by chromatography on silica gel (CH_2Cl_2/MeOH: (9.7:0.3)) to give compound **16** as a yellowish solid (80%). IR (film): γ = 3324, 2974, 2932, 1674, 1568, 1503, 1391, 1246, 1165 cm^{-1}. ^1H NMR (CD_3OD, 400 MHz): δ = 1.31−1.74 (m, 26H, 2 CH_2CH_2 and 2 $C(CH_3)_3$), 3.01 (t, 2H, ^3J = 6.7 Hz, $BocNHCH_2$), 3.19 (t, 2H, ^3J = 7.2 Hz), 3.24 (t-e, 2H), 3.51 (t, 2H, ^3J = 6.7 Hz, $CONHCH_2$), 7.16 (dd, 1H, ^3J = 7.6 Hz, ^4J = 1 Hz, H^7_{ar}), 7.42 (dd, 1H, ^3J = 8.2 Hz, ^4J = 1 Hz, H^5_{ar}), 7.53 (dd, 1H, ^3J = 8.2 Hz, ^3J = 7.6 Hz, H^6_{ar}), 8.18 and 8.39 (system AB, 2H, ^3J = 8.8 Hz, H^3_{ar} and H^4_{ar}) ppm. ^{13}C NMR (CD_3OD, 100 MHz): δ = 27.0 (2 CH_2), 27.9 (CH_2), 28.3 (CH_2), 28.7 ($C(CH_3)_3$), 28.8 ($C(CH_3)_3$), 40.3 (CH_2), 40.9 ($BocNHCH_2$), 48.1 (2 CH_2), 79.8 ($C(CH_3)_3$), 80.8 ($C(CH_3)_3$), 112.7 (C^7), 118.9 (C^5), 119.9 (C^4), 130.5 (C^6), 131.4 (C^{4a}), 138.4 (C^{8a}), 138.8 (C^3), 148.8 (C^2), 155.0 (C^8), 157.4 (C═O), 158.5 (C═O), 166.6 (CONH) ppm. HRMS (MALDI): calcd. for $C_{28}H_{42}N_4NaO_6$ $[M+Na]^+$; 553.2997; found 553.2971.

*N-[4-tert-Butyloxycarbonyl-(4-tert-butyloxycarbonyl-aminobutyl)aminobutyl]-8-hydroxyquinolin-2-carbo-thioamide (**17**).* To a stirred suspension of sulfur (1.6 equiv, 0.45 mmol as elemental sulfur) in dimethylformamide (1.5 mL) was added sodium sulfide (0.15 equiv, 0.042 mmol). The mixture was warmed until the solution appeared blue and was added via cannula to a stirring mixture of amine **1** (1 equiv, 0.28 mmol) and 2-formylquinolin-8-ol (1 equiv, 0.28 mmol) in dimethylformamide (1.5 mL) at 115 °C. After 2 h the mixture was quenched by addition of saturated ammonium chloride (20 mL) and extracted with diethyl ether. The organic extracts were dried over Na_2SO_4, filtered, and concentrated under reduced pressure and the residue was purified by chromatography on silica gel (CH_2Cl_2/EtOAc (9:1)) to give compound **17** as a yellow solid (52%). IR (film): γ = 3419, 3267, 2930, 1676, 1522, 1503, 1464, 1365, 1165 cm^{-1}. ^1H NMR (CD_3OD, 400 MHz): δ = 1.33−1.59 (m, 22H, CH_2CH_2 and 2 $C(CH_3)_3$), 1.62−1.73 (m, 2H), 1.78−1.88 (m, 2H), 3.00 (t, 2H, ^3J = 6.8 Hz, $BocNHCH_2$), 3.19 (t, 2H, ^3J = 6.8 Hz), 3.26 (t, 2H, ^3J = 6.8 Hz), 3.6 (t, 2H, ^3J = 6.8 Hz, $CSNHCH_2$), 7.16 (dd, 1H, ^3J = 7.6 Hz, ^4J = 1 Hz, H^7_{ar}), 7.40 (dd, 1H, ^3J = 8.2 Hz, ^4J = 1 Hz, H^5_{ar}), 7.51 (dd, 1H, ^3J = 8.2 Hz, ^3J = 7.6 Hz, H^6_{ar}), 8.32 and 8.80 (system AB, 2H, ^3J = 8.8 Hz, H^3_{ar} and H^4_{ar}) ppm. ^{13}C NMR (CD_3OD, 100 MHz): δ = 26.2 (CH_2), 27.1 (CH_2), 28.3 (2 CH_2), 28.7 ($C(CH_3)_3$), 28.8 ($C(CH_3)_3$), 41.0 ($BocNHCH_2$), 46.3 (CH_2), 48.1 (2 CH_2), 79.8 ($C(CH_3)_3$), 80.9 ($C(CH_3)_3$), 112.9 (C^7), 118.9 (C^5), 122.9 (C^4), 130.4 (C^6), 131.1 (C^{4a}), 137.3 (C^{8a}), 137.9 (C^3), 150.4 (C^2), 155.2 (C^8), 157.5 (C═O), 158.5 (C═O), 192.4 (CS) ppm. HRMS (MALDI): calcd. for $C_{28}H_{42}N_4NaO_5S$ $[M+Na]^+$; 569.2768; found 569.2775.

dx.doi.org/10.1021/bc4004734 | *Bioconjugate Chem.* 2014, 25, 320−334

*General Procedure for Boc Removal (**HQX-44**).* To a stirred solution of polyamines **9**, **15**−**17** (1 equiv, 0.2 mmol) dissolved in ethanol (2 mL) at 0 °C was added 6 M HCl (2 mL). After 12 h at room temperature, the solution was concentrated in vacuo and the resulting solid was washed with cold ethanol (−20 °C), filtered, and dried in vacuo to afford Quilamine **HQX-44** as a yellow solid (**HQ2**−**44**, **HQCO-44**), a white solid (**HQ0**−**44**), and an orange solid (**HQCS-44**), its hydrochloride salt.

*(2-[4-(4-Aminobutyl)aminobutyl]aminoethylquinolin-8-ol)ammonium Tetrachloride (**HQ2**−**44**).* (96%). Mp sup 250 °C. IR (KBr): γ = 2955, 2933, 2809, 2778, 2778, 1636, 1606, 1591, 1457, 1298, 838 cm^{-1}. ^1H NMR (D_2O, 400 MHz): δ = 1.79−1.95 (m, 8H, 2 CH_2CH_2), 3.07−3.23 (m, 6H, 3 CH_2), 3.25−3.33 (m, 2H, CH_2), 3.68−3.76 (m, 2H, CH_2), 3.77−3.86 (m, 2H, CH_2), 7.58 (dd, 1H, ^3J = 6.5 Hz, ^4J = 2.34 Hz, H^7_{ar}), 7.78−7.86 (m, 2H, H^5_{ar} and H^6_{ar}), 8.02 and 9.05 (system AB, 2H, ^3J = 8.4 Hz, H^3_{ar} and H^4_{ar}) ppm. ^{13}C NMR (D_2O, 100 MHz,): δ = 22.8 (3 CH_2), 23.9 (CH_2), 30.4 (CH_2), 38.9 (CH_2), 45.8 (CH_2), 46.8 (CH_2), 46.9 (CH_2), 47.3 (CH_2), 117.1 (C^7), 119.6 (C^5), 122.6 (C^3), 129.1 (C^{4a}), 129.9 (C^6), 130.4 (C^{8a}), 147.0 (C^4), 147.1 (C^2), 153.6 (C^8) ppm. HRMS (MALDI): calcd. for $C_{19}H_{31}N_4O$ $[M+H-4HCl]^+$; 331.2492; found 331.2497. Anal. Calcd. for $C_{19}H_{34}Cl_4N_4O{\cdot}0.25C_2H_6O{\cdot}0.95HCl$: C, 44.83; H, 7.03; N, 10.72. Found: C, 44.91; H, 6.97; N, 10.64.

*(2-[4-(4-Aminobutyl)aminobutyl]aminoquinolin-8-ol)-ammonium Trichloride (**HQ0**−**44**).* (95%). Mp sup 250 °C. IR (KBr): γ = 3461, 3104, 2935, 1669, 1608, 1570, 1467, 1281, 1219, 1050 cm^{-1}. ^1H NMR (D_2O, 400 MHz): δ = 1.64−2.11 (m, 8H, 2 CH_2CH_2), 3.05−3.33 (m, 6H, 3 CH_2), 3.65 (br t, 2H, CH_2), 7.00−7.16 (m, 1H), 7.24−7.32 (m, 1H), 7.38−7.51 (m, 2H), 8.22−8.31 (m, 1H) ppm. ^{13}C NMR (D_2O, 100 MHz,): δ = 22.8 (CH_2), 23.1 (CH_2), 23.9 (CH_2), 38.8 (CH_2), 41.5 (CH_2), 46.9 (CH_2), 47.2 (CH_2), 116.6 (2 C^{ar}), 119.7 (2 C^{ar}), 122.1, 125.6 (2 C^{ar}), 144.1, 152.4 ppm. HRMS (MALDI): calcd. for $C_{17}H_{27}N_4O$ $[M+H-3HCl]^+$; 303.2179; found 303.2183. Anal. Calcd. for $C_{17}H_{29}Cl_3N_4O.0.6C_2H_6O{\cdot}1.15HCl$: C, 45.41; H, 7.07; N, 11.64. Found: C, 45.42; H, 7.07; N, 11.64.

*(N-[4-(4-Aminobutyl)aminobutyl]-8-hydroxyquinolin-2-carboxamide)ammonium Trichloride (**HQCO-44**).* (98%). Mp sup 250 °C. IR (KBr): γ = 3444, 2351, 2976, 2859, 1678, 1596, 1537, 1440, 1296, 1143 cm^{-1}. ^1H NMR (D_2O, 400 MHz): δ = 1.73−1.91 (m, 8H, 2 CH_2CH_2), 3.03−3.23 (m, 6H), 3.48 (t, 2H, ^3J = 6.6 Hz, CH_2), 7.07 (dd, 1H, ^3J = 7.7 Hz, ^4J = 1.1 Hz, H^7_{ar}), 7.29 (dd, 1H, ^3J = 8.4 Hz, ^4J = 1.1 Hz, H^5_{ar}), 7.45 (dd, 1H, ^3J = 8.4 Hz, ^3J = 7.7 Hz, H^6_{ar}), 7.74 and 8.16 (system AB, 2H, ^3J = 8.8 Hz, H^3_{ar} and H^4_{ar}) ppm. ^{13}C NMR (D_2O, 100 MHz): δ = 22.7 (CH_2), 23.2 (CH_2), 23.9 (CH_2), 25.7 (CH_2), 38.8 (CH_2), 38.9 (CH_2), 46.8 (CH_2), 47.3 (CH_2), 112.2 (C^7), 118.3 (C^5), 118.9 (C^4), 129.4 (C^6), 129.5 (C^{4a}), 135.4 (C^{8a}), 138.4 (C^3), 145.8 (C^2), 150.9 (C^8), 165.5 (C═O) ppm. HRMS (MALDI): calcd. for $C_{18}H_{26}N_4NaO_2$ $[M+Na-3HCl]^+$; 353.1948; found 353.1942. Anal. Calcd. for $C_{18}H_{29}Cl_3N_4O_2.2.35H_2O$: C, 44.84; H, 7.05; N, 11.62. Found: C, 45.06; H, 7.05; N, 11.34.

*(N-[4-(4-Aminobutyl)aminobutyl]-8-hydroxyquinolin-2-carbothioamide)ammonium Trichloride (**HQCS-44**).* (94%). Mp sup 250 °C. IR (KBr): γ = 3431, 2958, 1569, 1522, 1502, 1386, 1275, 1156, 1087, 892 cm^{-1}. ^1H NMR (D_2O, 400 MHz): δ = 1.76−2.01 (m, 8H, 2 CH_2CH_2), 3.09 (t, 2H, ^3J = 6.9 Hz), 3.13−3.25 (m, 4H), 3.90 (t, 2H, ^3J = 6.9 Hz, CH_2), 7.05 (d, 1H, ^3J = 7.5 Hz, H^7_{ar}), 7.25 (d, 1H, ^3J = 8.3 Hz, H^5_{ar}), 7.42 (t, 1H, ^3J = 7.9 Hz, H^6_{ar}), 8.06 and 8.25 (system AB, 2H, ^3J = 8.4 Hz, H^3_{ar} and H^4_{ar}) ppm. ^{13}C NMR (D_2O, 100 MHz,): δ = 22.7 (CH_2), 23.5 (CH_2), 23.9 (CH_2), 24.2 (CH_2), 38.8 (CH_2), 45.1 (CH_2), 46.8 (CH_2), 47.3 (CH_2), 112.3 (C^7), 118.8 (C^5), 120.9 (C^4), 129.4 (C^6 and C^{4a}), 134.9 (C^{8a}), 137.4 (C^3), 148.1 (C^2), 151.4 (C^8), 190.5 (C═S) ppm. HRMS (MALDI): calcd. for $C_{18}H_{27}N_4OS$ $[M+H-3HCl]^+$; 347.1900; found 347.1897. Anal. Calcd. for $C_{18}H_{29}Cl_3N_4OS.0.3C_2H_6O.0.1H_2O$: C, 45.81; H, 6.78; N, 11.49; S, 6.57. Found: C, 45.56; H, 7.15; N, 11.09; S, 6.98.

Biological Methods. *Chelator Solutions.* All reagents, which were of the highest available grade, were obtained from Sigma-Aldrich (Saint Quentin Fallavier, France). All synthesized Quilamines were compared to the tridentate iron-chelator hydroxyphenyltriazole ICL670 as a reference (Deferasirox, Exjade from Novartis Pharma) as well as to 8-hydroxyquinoline. Stock solutions of each chelator (10 mM) were prepared in water. The high solubility of each derivative in culture medium in the concentration range 0−400 μM was first verified by turbidimetry measurement. Three controls were prepared for each experiment: one with the standard culture medium, and the other with culture medium.

Cell Selectivity for the PTS. The involvement of the PTS in the selective uptake of Quilamines was investigated by using Chinese Hamster Ovary cells (CHO) exhibiting high PTS activity[32] and the mutated derived-cell line CHO-MG cells, devoid of PTS (provided by Dr. W. Flintoff, University of Western Ontario).[33] The CHO-MG cells were selected for growth resistance to methylglyoxalbis-(guanylhydrazone), using a single-step selection after mutagenesis with ethyl methanesulfonate. Therefore, highly selective PTS ligands should give high (CHO-MG/CHO) IC_{50} ratios.

The two cell lines were grown in RPMI 1640 medium, supplemented with 10% fetal calf serum (Eurobio, Les Ulis, France), 2 mM glutamine (Bio Media, Boussens, France), 100 units/mL penicillin, and 50 μg/mL streptomycin, at 37 °C in 5% humidified CO_2. L-Proline (2 μg/mL) was added to the culture medium for CHO-MG cells.

Cell Treatment. Cells were harvested with trypsin and seeded for 24 h before polyamine treatment in 96-well microplates (Becton Dickinson, Oxnard, CA) at a density of 2000 cells per well. In these conditions, cells reached confluency in 5−6 days. Chelator exposure was performed one day after cell seeding in proliferating CHO and CHO-MG cells. To prevent oxidation of exogenous polyamine by the serum amine oxidase present in the fetal calf serum, aminoguanidine (1 mM), an inhibitor of this enzyme, was added to the medium. The various derivatives were compared to the tridentate iron chelator hydroxyphenyltriazole ICL670 (Deferasirox, Exjade) and to the bidentate 8-hydroxyquinoline.

Measurement of Cytostatic and Cytotoxic Effects. Chelator exposure was performed one day after cell seeding in proliferating CHO and CHO-MG cells. After 72 h of incubation at 37 °C, cell supernatants were collected for cytotoxicity analysis by measuring extracellular LDH activity (cytotoxicity detection kit − LDH, Roche, Penzberg, Germany). Extracellular LDH activity was measured as described by the manufacturer on a 20 μL aliquot of cell-free medium obtained by centrifugation (2500 rpm/min for 5 min). LDH activities were detected by reading absorbance at 485 nm. They were reported as a percentage of extracellular LDH activity with respect to the control value.

Cell viability was determined by counting the cell nuclei after staining with the fluorescent DNA intercalating dye Hoechst 33342. The treated CHO and CHO-MG cells were washed twice with PBS (50 mM pH 7) and fixed with ethanol/acetic acid for 20 min at 4 °C. Cells were counterstained for 10 min with Hoechst 33342 dye diluted by 1/1000 (5 μg/mL). Hoescht fluorescence (exc = 340 nm, em = 450 nm) was measured in a multiwell microplate fluorometer. The fluorescence intensity, which is proportional to the number of cell nuclei, was reported as a percentage of the control value. Parameters of the dose−response curves were deduced from a 4-parameter curve fit according to Rodbard[34]

$$y = \frac{(A_{cmin} - A_{cmax})}{1 + \left(\frac{C}{C_{ip}}\right)P_{ip}} + A_{cmax}$$

in which y is the percentage of the fluorescence intensity with respect to the control, $A_{C_{min}}$ and $A_{C_{max}}$ are the y values observed for minimal and maximal chelator concentrations, respectively, C is the chelator concentration (C_{ip} at the inflection point) and P_{ip} is the slope at the inflection point of the sigmoid curve. Due to their biphasic feature, the dose−response curves were fitted as the sum of two sigmoids (double 4-parameter fit). Percentages of cells involved in each viability response were deduced from the $A_{C_{min}}$, $A_{C_{max}}$, and IC_{50} values of each sigmoid, which were obtained from these fits.

Three independent replicates were performed for each experiment, which was repeated three times.

Screening of the Cytostatic/Cytotoxic Effects in Tumor Cell Lines. The various derivatives were compared to the tridentate iron chelator hydroxyphenyltriazole ICL670 (Deferasirox, Exjade) and to the bidentate 8-hydroxyquinoline.

The cytostatic and cytotoxic effects of Quilamines were tested on various cell lines from human tumors and obtained from the ECACC collection. They included HuH7 (hepatocarcinoma), Caco-2 and HCT-116 (colon cancers), MDA-MB231 (breast cancer), PC3 (prostate cancer), NCI-H727 (lung cancer), and Hacat, a human immortalized keratinocyte cell line. These cells were grown according to ECACC recommendations. This study was extended to skin diploid fibroblastic cells which were provided by BIOPREDIC International Company (Rennes, France).

The cytostatic/cytotoxicity tests of the compounds on these cells were as follows: 2.103 cells/well for the HCT-116 cell line or 4.103 cells/well for the other cell lines were seeded in 96-well microplates (Becton Dickinson, Oxnard, CA). In these conditions, cells reached confluency in 5−6 days. Twenty-four hours after seeding, cells were exposed to increasing concentrations of the compounds (0.1−200 μM). To prevent oxidation of exogenous polyamine by the serum amine oxidase present in the fetal calf serum, aminoguanidine (1 mM), an inhibitor of this enzyme, was added to the medium. After 48 h of treatment, 20 μL of cell supernatants were collected for cytotoxicity analysis by measuring extracellular LDH activity (see above).

Cell viability was determined by counting the cell nuclei after staining with the fluorescent DNA intercalating dye Hoechst 33342 as described above. Fits of the dose−effect curves were performed as described above and percentages of cells involved in each viability responses were deduced from the $A_{C_{min}}$, $A_{C_{max}}$, and IC_{50} values of each sigmoid, which were obtained from these fits.

Three independent replicates were performed for each experiment, which was repeated three times.

Physicochemical Methods. *Comparison of Chelator Efficiency in the Aqueous Phase and Competition with Calcein.* In solution, calcein, a fluoresceinated analogue of EDTA, binds iron(II) and, more slowly, iron(III).[35] The fluorescence of this metallosensor dye is quenched during its interaction with iron and, conversely, is restored if iron is removed from the [calcein-iron] complex by a more efficient competitive iron chelator. The rate and extent of fluorescence recovery depend on the chelator concentration, the kinetics and stoichiometry of iron binding, and the relative binding affinity.

The fluorescence emission (λ_{Exc} = 485 nm, λ_{Em} = 520 nm) of calcein (100 nM) in a HEPES buffer (20 mM HEPES, 150 mM NaCl, pH 7.3) was measured at room temperature in a microplate fluorescence reader (Polarstar Omega, BMG Labtech), equipped with orbital stirring. Iron(III) (1 μM) slowly reacted with calcein and maximal quenching of its fluorescence was observed at a time longer than 6 h. The fluorescence recovery was monitored after 4 h incubation in the presence of various chelator concentrations. In the absence of iron, some chelators slightly modulated the calcein fluorescence intensity. The results were expressed as a percentage of fluorescence recovery with respect to the free calcein fluorescence intensity measured in the absence of iron. The calcein test is qualitative, but the concentration of the chelator for which 50% of the fluorescence is restored is indicative of chelator affinity (RC_{50}). These RC_{50} values were deduced from the four-parameter curve fitting of the dose−effect curves.

HVA Assay. We have previously developed a simple, sensitive, and reliable test to measure the total antioxidative efficiency of biological fluids.[36] The autoxidation of homovanillic acid (HVA) gives rise to a fluorescent dimer ($\lambda_{exc.}$= 315 nm; λ_{em} = 425 nm). Its appearance, monitored by its fluorescence increase, follows a linear kinetic pattern for a time longer than 5 h. This Fenton-like reaction, which requires divalent metal ions such as Fe^{2+}, can be transiently stopped by various ROS scavengers inducing a delay in the HVA autoxidation. In contrast, metal chelating agents such as 8-hydroxyquinoline (HQ) and Quilamines only reduce the HVA autoxidation rate without introducing a detectable delay. These characteristics constitute the basis of the HVA test which enables, in a single run, the investigation of both components of the antioxidant property: ability to prevent the formation of ROS by chelation and/or to scavenge the free radicals giving rise to HVA autoxidation.

The final reaction mixture for the HVA assay contained 3×10^{-4} M HVA in 0.1 M borate buffer (pH 9.0). Quilamines, at various final concentrations ranging from 0 to 200 μM, were introduced in 200 μL of this reaction mixture in a 96-well microplate. They were incubated at 37 °C under gentle stirring and fluorescence was measured every minute ($\lambda_{exc.}$ = 340 nm; λ_{em} = 440 nm) using a microplate fluorescence reader (Polarstar Omega, BMG Labtech). The autoxidation level in the absence (R_0) or presence of an effector (R_a) was calculated from the slope of the fluorescence kinetics. Each kinetic determination was performed in triplicate.

RESULTS AND DISCUSSION

Chemistry. As for the first-generation Quilamines, the synthesis of ligand **HQ2−44** was envisaged by a reductive

dx.doi.org/10.1021/bc4004734 | Bioconjugate Chem. 2014, 25, 320−334

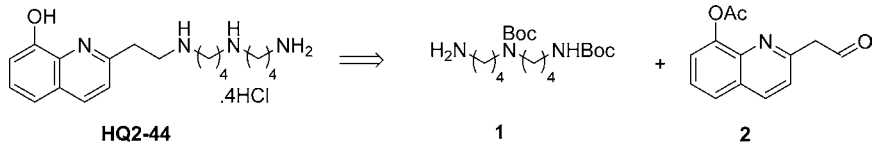

Figure 3. Retrosynthesis of Quilamine **HQ2−44**.

Scheme 1. Synthesis of Protected Homospermidine 1[a]

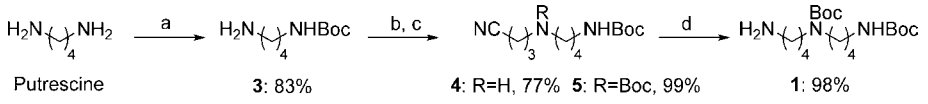

[a]Reagents: (a) $(Boc)_2O$ (0.33 equiv), Et_3N, MeOH, 0 °C to r.t., 20 h; (b) 4-bromobutyronitrile (1 equiv), K_2CO_3, CH_3CN, 50 °C, 12 h; (c) $(Boc)_2O$ (2.5 equiv), Et_3N, MeOH, r.t., 20 h; (d) H_2, Raney Ni, EtOH, NH_4OH, 20 atm, r.t., 12 h.

Scheme 2. Synthesis of 2-(8-Hydroxyquinolin-2-yl)acetaldehyde 2[a]

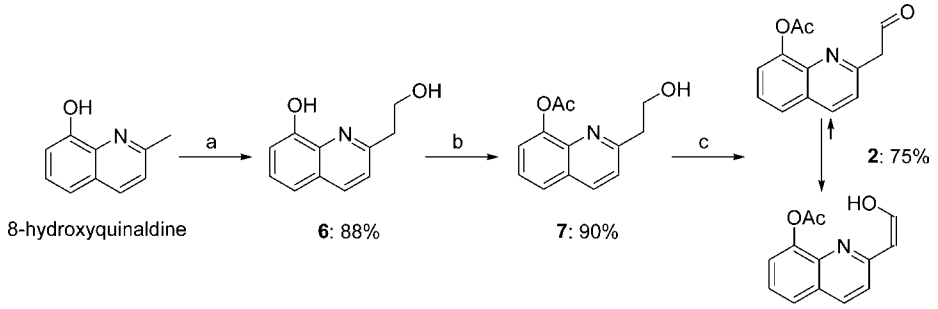

[a]Reagents: (a) *n*BuLi (2.2 equiv), paraformaldehyde (4 equiv), THF, −78 °C to r.t., 3 h; (b) $(CH_3CO)_2O$ (1.2 equiv), NaOH 1 M, CH_2Cl_2, r.t., 3 h; (c) $(COCl)_2$ (1.2 equiv), DMSO (2.4 equiv), Et_3N (4.8 equiv), CH_2Cl_2, −78 °C to r.t., 2 h.

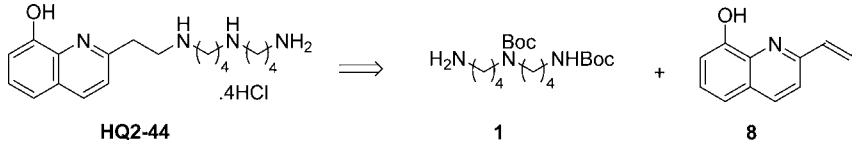

Figure 4. Retrosynthesis of Quilamine **HQ2−44**.

amination between the protected homospermidine **1** and the protected 2-(8-hydroxyquinolin-2-yl)acetaldehyde **2** (Figure 3).

The homospermidine analogue **1** was prepared according to a modified four-step procedure providing good yields (Scheme 1).[31] The first step consisted of reacting putrescine with di-*tert*-butyl dicarbonate (Boc_2O) leading to monoprotected diamine **3**, which was reacted with 4-bromobutyronitrile to give secondary amine **4**, followed by quantitative Boc-protection giving rise to compound **5**. The nitrile was reduced by hydrogenation with Raney Ni to give masked homospermidine **1** with an overall yield of 63%.[21,37]

The synthesis of aldehyde **2** was carried out in three steps from commercial 8-hydroxyquinaldine with an overall yield of 60% (Scheme 2). 2-(2-Hydroxyethyl)quinolin-8-ol **6** was obtained by hydroxymethylation of 8-hydroxyquinaldine, using *n*-butyl lithium in THF in the presence of paraformaldehyde as an electrophile to trap the anion formed.[38] The hydroxyl of phenol **6** was then protected in acetate form, in the presence of acetic anhydride in a two-phase volume to volume solution of dichloromethane and an aqueous solution of 1 M sodium hydroxide, to lead to product **7**. Finally, the primary alcohol function of compound **7** was oxidized in Swern conditions to give acetaldehyde **2** which tautomerizes with the enol form.

The reductive amination of this aldehyde **2** with homospermidine **1** was achieved in one pot by using sodium triacetoxyborohydride to reduce the imine generated in situ.[39] Unfortunately, it proved impossible to form the expected compound, and only the product of the deprotection of the phenol function could be recovered at the end of the reaction. This lack of reactivity may be due to the strong stabilization of the enol form by hydrogen bonding between the enol, the nitrogen of pyridine and acetate. In fact, NMR analysis revealed that the enol is by far the major form in solution (90/10). The hydrogen of the hydroxyl group has a chemical shift of 15 ppm, which appears as a broad singlet even in polar solvents, while the ethylenic hydrogens have a low coupling constant ^3J of 3.2 Hz, characteristic of the Z geometry of the double bond. Lastly, a DEPT analysis showed that no CH_2 was present in the structure.

The synthesis of Quilamine **HQ2−44** was thus envisaged by Michael addition between homospermidine **1** and 2-vinylquinolin-8-ol **8** (Figure 4).

2-Vinylquinolin-8-ol **8** was synthesized by intramolecular dehydration of alcohol **6**. Following this reaction, the use of 2 equiv of methanesulfonyl chloride, in the presence of triethylamine in dichloromethane at room temperature, protected the phenolic hydroxyl and activated the primary

dx.doi.org/10.1021/bc4004734 | *Bioconjugate Chem.* 2014, 25, 320−334

alcohol. Basic treatment of this intermediate led simultaneously to the deprotection of the phenol group and the elimination of methanesulfonic acid thus giving the desired vinylic compound **8** in 96% yield (Scheme 3). This strategy proved to be much

Scheme 3. Synthesis of 2-Vinylquinolin-8-ol 8[a]

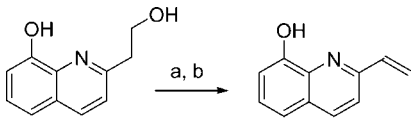

6 **8**: 96%

[a]Reagents: (a) MsCl (3 equiv), Et_3N (5 equiv), CH_2Cl_2, r.t., 2 h; (b) NaOH (1 M), EtOH, reflux, 4 h.

more efficient than the method described by Yoneda who obtained 2-vinylquinolin-8-ol **8** by a Wittig reaction between 2-formylquinolin-8-ol and methyltriphenylphosphonium bromide with a yield of only 30%.[40]

Homospermidine **1** was then reacted with vinyl **8** in a Michael addition carried out in methanol, in the presence of a catalytic quantity of acetic acid, which led to the formation of compound **9** with a yield of 64%. Deprotection of amines by aqueous hydrochloric acid in ethanol at room temperature resulted in the formation of Quilamine **HQ2−44**, in hydrochloride form (Scheme 4).

For Quilamine **HQ0−44**, we envisaged a reductive amination between commercial 2-aminoquinolin-8-ol and homospermidine **10** carrying an aldehyde function at the end of the chain obtained by reduction of compound **5** (Figure 5).

Different attempts were made to reduce polyaminonitrile **5** by diisobutylaluminum hydride by varying the temperature of the reaction (from −78 °C to room temperature) or the number of reductor equivalents (from 1 to 3) but aldehyde **10** was never obtained. Treatment with sodium hypophosphite and Raney nickel was also unsuccessful.[41,42] So was the last method we tried which was based on the reduction of nitrilium ion by triethylsilane.[43] We thus changed strategy and opted for the synthesis of aldehyde **10** by oxidation of the corresponding alcohol (Scheme 5).

The nitrogen atom of 4-aminobutan-1-ol was monoalkylated by 4-bromobutanenitrile in acetonitrile in the presence of potassium carbonate, at a temperature which must not exceed 50 °C to avoid disubstitution (monitored by TLC). Amine **11** was protected by a Boc group in order to isolate compound **12**. The latter was hydrogenated under a pressure of 20 bar in the presence of Raney nickel and ammonium hydroxide in ethanol leading to aminoalcohol **13**.[44] A new protection of the amine function gave alcohol **14**. Oxidation of the hydroxyl in aldehyde **10** was first attempted in Swern conditions or with pyridinium chlorochromate, but only degradation products were recovered at the end of the reaction. In contrast, when a catalytic quantity of (2,2,6,6-tetramethylpiperidin-1-yl)oxyl (TEMPO) was used as oxidant and of bis(acetoxy)iodobenzene (BAIB) as co-oxidant, aldehyde **10** was isolated in good yield (75%).[45]

The reductive amination of this aldehyde with 2-aminoquinolin-8-ol was achieved in one pot by using sodium triacetoxyborohydride to reduce the imine generated in situ. Protected intermediate **15** was isolated in good yield (73%) and removal of the Boc-protecting groups under acidic conditions at room temperature gave Quilamine **HQ0−44** as the hydrochloride salt (Scheme 6).

The second modification envisaged concerned the nature of the spacer, i.e., the introduction of a carbonyl (**HQCO-44**) and a thiocarbonyl (**HQCS-44**) between homospermidine and hydroxyquinoline.

Protected Quilamine **HQCO-44** (**16**) was obtained in 80% yield by peptide linkage between homospermidine **1** and commercial 8-hydroxyquinaldinic acid in the presence of *N*,*N*′-dicyclohexylcarbodiimide (DCC) and hydroxybenzotriazole (HOBt) in dichloromethane (Scheme 7). Deprotection of the amine functions of compound **16**, by aqueous hydrochloric acid in ethanol, led to Quilamine **HQCO-44** as the hydrochloride salt.

For Quilamine **HQCS-44**, the most obvious strategy is to carry out a sulfuration of Quilamine **HQCO-44**. With this aim, we began with amide **16** to obtain the corresponding thioamide **17**. Different attempts were made by varying the sulfuration reagent (Lawesson's reagent (LR), phosphorus pentasulfide, Davy's reagent), the nature of the solvent (toluene, tetrahydrofuran), and the temperature (from room temperature to reflux). Unfortunately, regardless of the experimental conditions used, thioamide **17** could not be obtained and only an extremely insoluble salt was recovered. Several attempts at sulfuration were also carried out by first protecting phenol with different groups (acetate, ether, sulfonate), but only the deprotection products were recovered at the end of the reaction and the use of an excess of sulfuration reagent proved ineffective.

Kanbara has recently described the formation of several thioamides from aldehydes and aromatic amines using the Willgerodt-Kindler reaction.[46] Sulfur was used as the sulfuration agent and a catalytic quantity of sodium sulfide was introduced as a base in order to start the reaction.[47] By applying these experimental conditions, we obtained the desired thiocarbonylated derivative **17** starting from commercial 2-formylquinolin-8-ol and homospermidine **1** (Scheme 8). As for the other Quilamines, thioamide **17** was deprotected to afford Quilamine **HQCS-44** as the hydrochloride salt.

These four new second-generation Quilamines were fully characterized by a combination of the usual techniques (IR, MS, elemental analysis, ^{13}C and ^{1}H NMR) and fulfilled the required purity for the biological evaluations.

Biological Evaluations. *Selectivity for the Polyamine Transport System (PTS).* This second generation of Quilamines, HQX-44 (**HQ2−44**, **HQ0−44**, **HQCO−44**, and **HQCS−44**) were screened for their antiproliferative activity

Scheme 4. Synthesis of Quilamine HQ2-44[a]

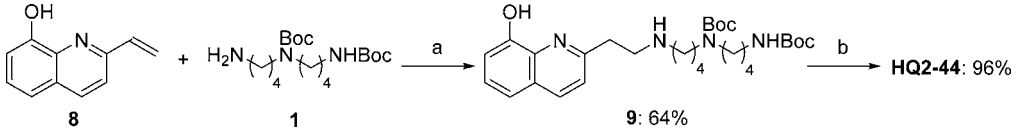

8 **1** **9**: 64%

[a]Reagents: (a) AcOH (cat), MeOH, 70 °C, 24 h; (b) HCl (6 M), EtOH, r.t., 12 h.

dx.doi.org/10.1021/bc4004734 | *Bioconjugate Chem.* 2014, 25, 320−334

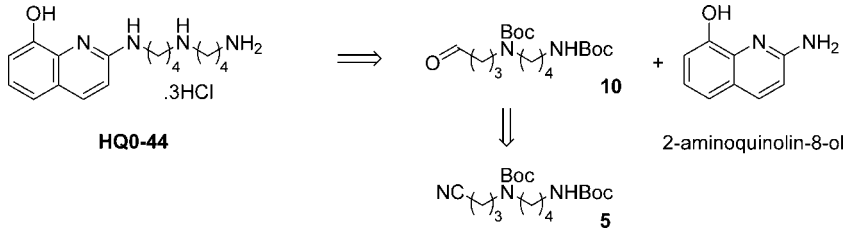

Figure 5. Retrosynthesis of Quilamine **HQ0−44**.

Scheme 5. Synthesis of Aldehyde 10[a]

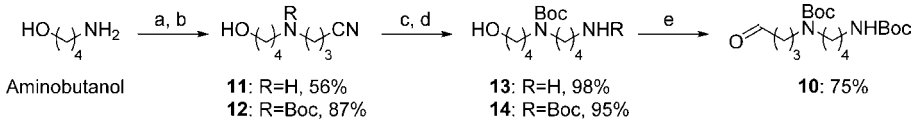

[a]Reagents: (a) 4-bromobutyronitrile (1 equiv), K_2CO_3 (1.5 equiv), CH_3CN, 50 °C, 12 h; (b) $(Boc)_2O$ (1.5 equiv), Et_3N, MeOH, r.t., 24 h; (c) H_2, Raney Ni, EtOH, NH_4OH, 20 atm, r.t., 12 h; (d) $(Boc)_2O$ (2 equiv), Et_3N, MeOH, r.t., 24 h; (e) TEMPO (0.1 equiv), BAIB (1.1 equiv), CH_2Cl_2, r.t., 5 h.

Scheme 6. Synthesis of Quilamine HQ0-44[a]

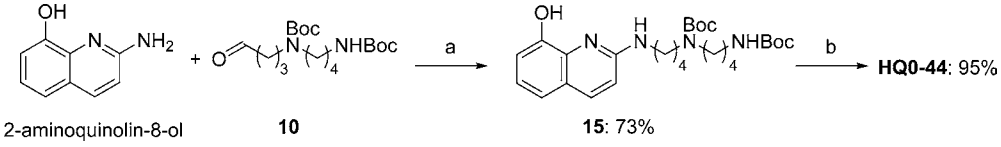

[a]Reagents: (a) $NaBH(OAc)_3$ (3 equiv), $C_2H_4Cl_2$, r.t., 12 h; (b) HCl (6 M), EtOH, r.t., 12 h.

Scheme 7. Synthesis of Quilamine HQCO-44[a]

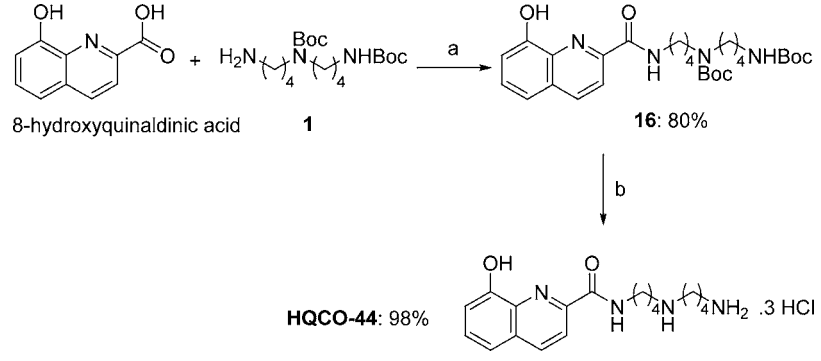

[a]Reagents: (a) DCC (1.1 equiv), HOBt (1.1 equiv), CH_2Cl_2, r.t., 20 h; (b) HCl (6 M), EtOH, r.t., 12 h.

Scheme 8. Synthesis of Quilamine HQCS-44[a]

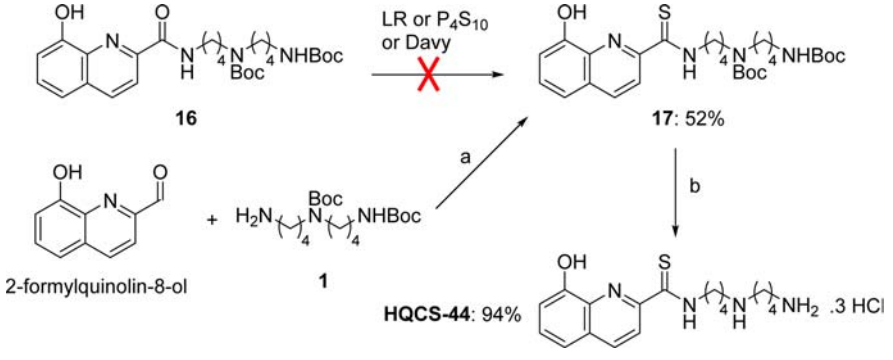

[a]Reagents: (a) S_8 (1.6 equiv), Na_2S (0.15 equiv), DMF, 115 °C, 2 h; (b) HCl (6 M), EtOH, r.t., 12 h.

dx.doi.org/10.1021/bc4004734 | *Bioconjugate Chem.* 2014, 25, 320−334

and cytotoxicity in CHO (Chinese Hamster Ovary) cells, which exhibit high PTS activity,[48] and the mutated derived-cell line CHO-MG cells, devoid of the PTS (provided by Dr. W. Flintoff, University of Western Ontario).[33] CHO cells and the CHO-MG cell line were chosen to evaluate the potential role of the PTS as a selective transport system. We assessed the antiproliferative activity of the various compounds by measuring DNA content after Hoescht staining. The dose–effect curves reflected both the PTS efficiency and the cytostatic/cytotoxic effects of each compound. The release of the cytoplasmic protein lactate dehydrogenase (LDH) into cell supernatants was used as a marker of cell membrane disruption correlated to cytotoxicity. The IC_{50} values obtained by fitting the dose–effect curves are recorded in Table 1. In this study, 8-hydroxyquinoline and ICL670 (tridentate iron chelator, Deferasirox, Exjade from Novartis Pharma) were used as reference chelators, while Quilamine **HQ1–44** was introduced to compare the activities of second-generation Quilamines.

Table 1. Selectivity of Quilamines for the PTS[a]

	IC_{50} (μM)		IC_{50} ratio[a]
Compound	CHO	CHO-MG	CHO-MG/CHO
HQ1–44	1.4	344.5	249
HQ2–44	1.8	>800	>500
HQ0–44	0.4	130	325
HQCO–44	35	>800	>30
HQCS–44	25	140	5.6
8-HQ	5.0	6.5	1
ICL670	9.2	8.0	1

[a]Effect of Quilamines HQX-44, 8-HQ, and ICL670 on cell viability in CHO and CHO-MG cells. [a]This denotes the (CHO-MG/CHO) IC_{50} ratio, a measurement of PTS selectivity.

Quilamines differing in the length of the spacer (**HQ0–44**, **HQ1–44**, and **HQ2–44**) showed increased antiproliferative activities, with IC_{50} values between 0.4 and 1.8 μM, while those differing in the chemical nature of the spacer (**HQCO-44** and **HQCS-44**) were less effective, with higher IC_{50} values. A weaker effect of all the Quilamines on the proliferation of CHO-MG cells was observed with IC_{50} values ranging from 130 to more than 800 μM (Table 1). These results are consistent with a low uptake of Quilamines into CHO-MG cells and thus a weak activity in the absence of the PTS. The reference chelators, 8-hydroxyquinoline and ICL670, with no polyamine vector, enter cells by a route other than the PTS and thus presented identical IC_{50} values for both CHO and CHO-MG cells.

The ratio between the IC_{50} obtained for the CHO-MG and CHO cell lines gives an indication of the degree of selectivity of uptake by the PTS (Table 1). Two groups of Quilamines can be clearly distinguished: Quilamines **HQCO-44** and **HQCS-44** with an IC_{50} ratio between 1 and 30, implying an average selectivity for the PTS; and Quilamines **HQ0–44**, **HQ1–44**, and **HQ2–44** with an IC_{50} ratio higher than 200, indicating strong selectivity for the PTS.

Thus, although they contain the same polyamine vector (homospermidine chain), the second-generation Quilamines display differences in selectivity for the PTS. Changing the size of the spacer increased the selectivity while a decrease in selectivity was observed when its chemical nature was changed. Several factors can explain these results.

Studies carried out by Phanstiel and Delcros using anthracene–polyamine and naphthalene–polyamine derivatives showed that the charge and the size of polyamines were key parameters for the synthesis of compounds targeting the PTS.[27,28] They put forward a model enabling the design of cytotoxic N^1-substituted triamines specifically targeting the PTS (Figure 6).[49] Their work showed that the best selectivity was obtained with triamines having butyl or pentyl chains between the N^1 and N^2 nitrogen atoms, and propyl or butyl chains between the N^2 and N^3 nitrogen atoms. In fact, this model shows three negative charges (probably amino acids deprotonated at physiological pH) at the PTS level with a spacing corresponding to that of the alkyl chains between the nitrogen atoms of the triamine (Figure 6). Moreover, the size of the spacer between the N^1 nitrogen and the substituent R also plays a role in the selectivity. These authors suggested the presence of a hydrophobic pocket within the recognition site of the PTS which would favor affinity (Figure 6). Bergeron finally confirmed these results in a study of the vectorization of iron chelators by polyamines, in which he also showed that the charge of the chelating group was an essential factor.[50,51]

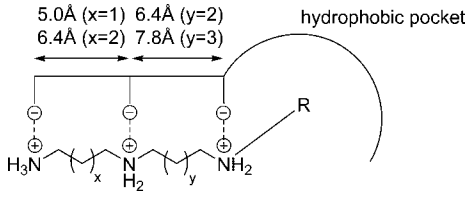

Figure 6. Model of the structural constraints of the PTS proposed by Phanstiel and Delcros.[49]

This model could explain the drop in selectivity observed for Quilamines **HQCO-44** and **HQCS-44** in relation to other Quilamines. Indeed, the introduction of carbonyl and thiocarbonyl groups prevents the nitrogen of the (thio)amide function from being protonated at physiological pH. Thus, the loss of an electrostatic interaction, required for recognition, could be the reason for the decreased affinity of these Quilamines for the PTS (Figure 7).

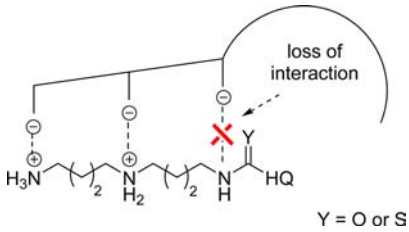

Figure 7. Hypothesis to explain the loss of selectivity of Quilamines **HQCO-44** and **HQCS-44** for the PTS according to the model of Phanstiel and Delcros.[49]

Quilamine **HQ0–44** has an amidine function within its structure. At physiological pH, this function is monocationic with a distribution of the positive charge between the two nitrogen atoms. This delocalization could be responsible for a higher electrostatic interaction and thus a gain in selectivity (Figure 8, left). Assuming that there is a hydrophobic pocket within the PTS structure, increasing the size of the spacer in Quilamine **HQ2–44** could result in the heterocycle being

dx.doi.org/10.1021/bc4004734 | Bioconjugate Chem. 2014, 25, 320–334

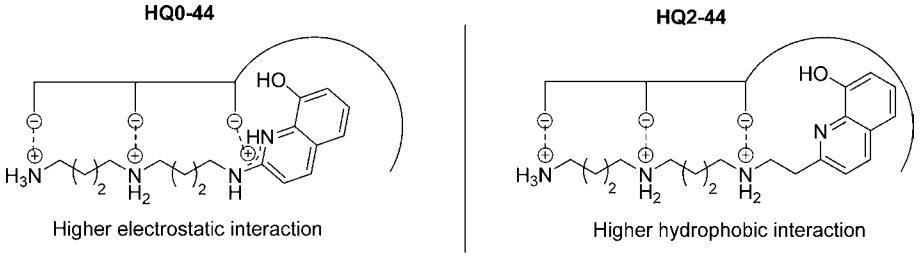

Figure 8. Hypothetical modeling of the structure−selectivity relationship between the PTS and Quilamines **HQ0−44** and **HQ2−44** according to the model of Phanstiel and Delcros.[49]

closer to this cavity, thus increasing its interaction (Figure 8, right).

Taken together, our data suggest that changes made to the size of the spacer have improved the selectivity of Quilamines for the PTS unlike those made to the nature of the spacer.

*Antiproliferative Action of Quilamines **HQ0−44**, **HQ1−44**, and **HQ2−44** on Human Tumor Cell Lines.* In this work, as the antiproliferative activity of Quilamines **HQCO-44** and **HQCS-44** was shown to be low (Table 1), only **HQ0−44** and **HQ2−44** were assessed on different human tumor cell lines and compared to **HQ1−44** as a biological activity reference.

The dose−effect curves, like that obtained after treatment of HCT-116 cells by **HQ1−44** presented in Figure 9, can be

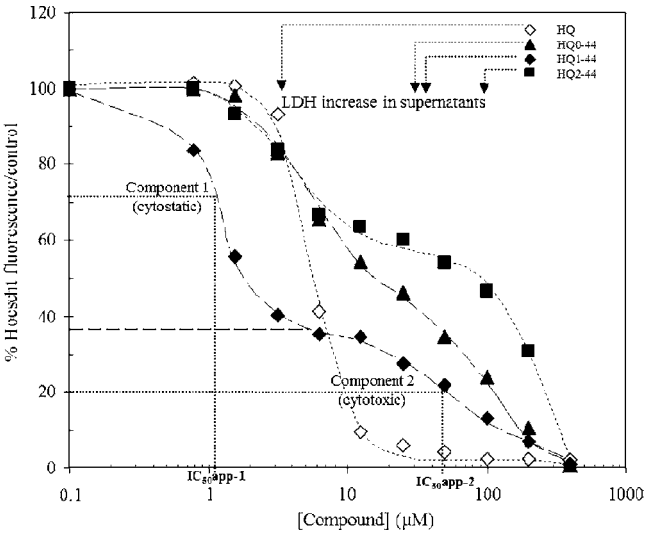

Figure 9. Cytostatic and cytotoxic effects of Quilamines **HQ0−44** (—▲—), **HQ1−44** (- -♦- -), and **HQ2−44** (- -■- -) compared to the reference chelator 8-hydroxyquinoline, **HQ** (—◇—). The effect on cell viability was determined by measuring DNA content after Hoescht staining and fluorescence analysis. The cytotoxic effect leading to cell membrane damage was evaluated by measuring LDH leakage into the cell supernatant. The arrows indicate the minimum Quilamine concentration triggering a rise in LDH activity compared to the untreated control.

parametrized into two components. The first indicates the antiproliferative effect of the Quilamine (component 1, C1, cytostatic) and the second its cytotoxicity (component 2, C2, cytotoxic), linked to membrane damage leading to a release of lactate dehydrogenase (LDH) into the supernatant. The viability curves of Quilamines **HQ0−44**, **HQ1−44**, and **HQ2−44** were compared in the HCT116 cell line to that of the reference iron chelator 8-hydroxyquinoline (**HQ**). The dose−effect curves reported in Figure 9 were shown to be biphasic for the three Quilamines with a cytostatic effect in the concentration range 1−5 μM and a cytotoxic effect at higher concentration marked by arrows in the figure. In contrast, only one cytotoxic effect was observed with the reference chelator **HQ**.

The percentages of each of these two components and their apparent IC_{50} values (IC_{50app}-1 and IC_{50app}-2), calculated from a sigmoid fit of the curves, are given in Table 2. The minimum Quilamine concentration triggering a rise in LDH release compared to the control is also given.

As for Quilamine **HQ1−44**, CHO cells, which have the most effective PTS, show the highest percentage of antiproliferative component (C1) after treatment with Quilamines **HQ0−44** and **HQ2−44**. For MDA, NCI-H727, and PC3 cells, the three Quilamines exhibit no antiproliferative effect and only their cytotoxicity is observed at higher concentrations.

The antiproliferative effect of Quilamines is most marked on HCT-116, HuH7, and Caco-2 cell lines, which show component C1 percentages between 14% (**HQ0−44**, Caco-2) and 62% (**HQ1−44**, HCT-116) and IC_{50app}-1 values between 1.3 μM (**HQ1−44**, HCT-116) and 5 μM (**HQ0−44**, HCT-116). HCT-116 cells respond most effectively to Quilamine **HQ1−44** (component **1** of 62% and IC_{50app}-1 of 1.3 μM) while for Caco-2, HuH7, and Hacat cells, the first component only represents 35%, 30%, and 25%, respectively, of the total effect. In contrast, the low antiproliferative component observed for fibroblasts (25%), along with a higher IC_{50app}-1 of 7.5 μM, demonstrates the weak activity of Quilamine **HQ1−44** on nontransformed cells.

The toxicity of Quilamines **HQ0−44** and **HQ2−44** seems more marked than that of **HQ1−44**. In fact, for CHO cells, the antiproliferative components of the three Quilamines are of the same order (about 80%), but the minimum concentration triggering a rise in LDH activity compared to the control (membrane damage) is observed at lower concentrations of 1.5 and 10 μM for Quilamines **HQ0−44** and **HQ2−44**, respectively, while Quilamine **HQ1−44** is not toxic below 30 μM. Thus, these three Quilamines clearly present a marked antiproliferative effect, but the difference in their toxicity suggests that other phenomena are involved for each molecule.

In addition, the antiproliferative effect seems different between the three Quilamines as they present different percentages of component **1** for the lines studied. For example, for Caco-2 cells, Quilamines **HQ0−44**, **HQ1−44**, and **HQ2−44** have a component **1** representing 14%, 35%, and 50%, respectively, of the total effect. This is consistent with these three Quilamines having different modes of action within the cell.

Physicochemical Evaluations. *Calcein Assay.* The cellular labile iron pool (LIP) consists of chelatable and redox-active iron, which plays a key role as a crossroads of cell

dx.doi.org/10.1021/bc4004734 | *Bioconjugate Chem.* 2014, 25, 320−334

Table 2. Percentages of the Two Components and Apparent IC_{50} Values Calculated for Quilamines HQ0-44, HQ1-44, and HQ2-44 on Different Human Cell Lines[a]

	HQ0−44			HQ1−44			HQ2−44		
cell lines	%C1	IC_{50app}-1 (μM)	LDH[b] (μM)	%C1	IC_{50app}-1 (μM)	LDH[b] (μM)	%C1	IC_{50app}-1 (μM)	LDH[b] (μM)
CHO	85	0.4	1.5	85	1.2	30	83	1.4	10
HCT-116	55	5	30	62	1.3	30	36	5	100
HuH7	18	5	22	30	2.7	66	25	15	200
Caco-2	14	1	66	35	4	66	50	2	66
Fibroblast	25	7.5	66	25	7.5	66	25	15	66
Hacat	N.D.	N.D.	22	25	1.5	22	25	1.5	200
MDA	N.D.	N.D.	22	N.D.	N.D.	66	N.D.	N.D.	200
NCI-H727	N.D.	N.D.	66	N.D.	N.D.	66	N.D.	N.D.	22
PC3	N.D.	N.D.	22	N.D.	N.D.	66	N.D.	N.D.	200

[a]N.D.: not detectable. [b]Minimum Quilamine concentration triggering a rise in LDH activity compared to the untreated control.

iron metabolism. The ability of iron chelators to mobilize this temporary iron pool bound to low molecular weight and low iron affinity chelators (citrate, ascorbate, phosphate, and adenosine triphosphate) is an essential factor influencing their biological efficiency. According to previous work, the calcein test can predict the iron-chelating efficiency of chelators.[52,53] Thus, an acellular calcein test was performed to compare the potential ability of Quilamines bearing various chain length linkers, **HQ0−44**, **HQ1−44**, **HQ2−44**, and the reference iron chelator 8-hydroxyquinoline (**HQ**), to chelate this labile iron pool at physiological pH. Recovered calcein fluorescence was measured 4 h after the addition of the competitive chelators and is reported as a function of their concentrations in Figure 10A. As previously reported,[31] we confirmed the chelating efficiency of Quilamine **HQ1−44** (RC_{50} = 1 μM) is higher than that of the reference chelator, **HQ** (RC_{50} = 3.7 μM). The ability of Quilamine **HQ2−44** (RC_{50} = 3 μM) to transchelate iron from calcein was similar to that of 8-hydroxyquinoline while that of **HQ0−44** was lower (RC_{50} = 7.5 μM). Due to their amino groups, polyamines are also able to chelate metallic cations.[54,55] The stability constants of these chelates increase with the number of amino groups and with the chain length of the polyamine.[56] Our previous results suggested the involvement of the amine group of the polyamine chain in the formation of iron complexes, as expected during the design and synthesis of this Quilamine concept.[31] Our present study showed that the involvement of the first secondary amine in Quilamines, in iron coordination, depended on the chain length of the linker. When this amine was directly connected to the hydroxyquinoline moiety (**HQ0−44**), the compound was fluorescent and its chelating capacity was lower than that of the reference chelator **HQ**. When this amine was linked by a longer spacer (2 carbon atoms) to the chelating moiety, it did not appear to be involved in iron coordination, since the chelating ability of **HQ2−44** was shown to be similar to that of **HQ**. With an intermediary chain length spacer of one carbon atom, our results suggested the involvement of the first amine in iron coordination. So, **HQ1−44** could exhibit the best iron transchelating ability from calcein which could explain its higher cytostatic effect.

HVA Assay. The effects of Quilamines and **HQ** on HVA autoxidation are shown in Figure 10B. None of these Quilamines induced a delay in the autoxidation reaction, but all of them induced a significant decrease in the autoxidation level in relation to their concentration. This behavior is characteristic of metal chelating agents with very low (or no) scavenging capability against the ROS (mainly the hydroxyl radicals) involved in the HVA oxidation process.[36]

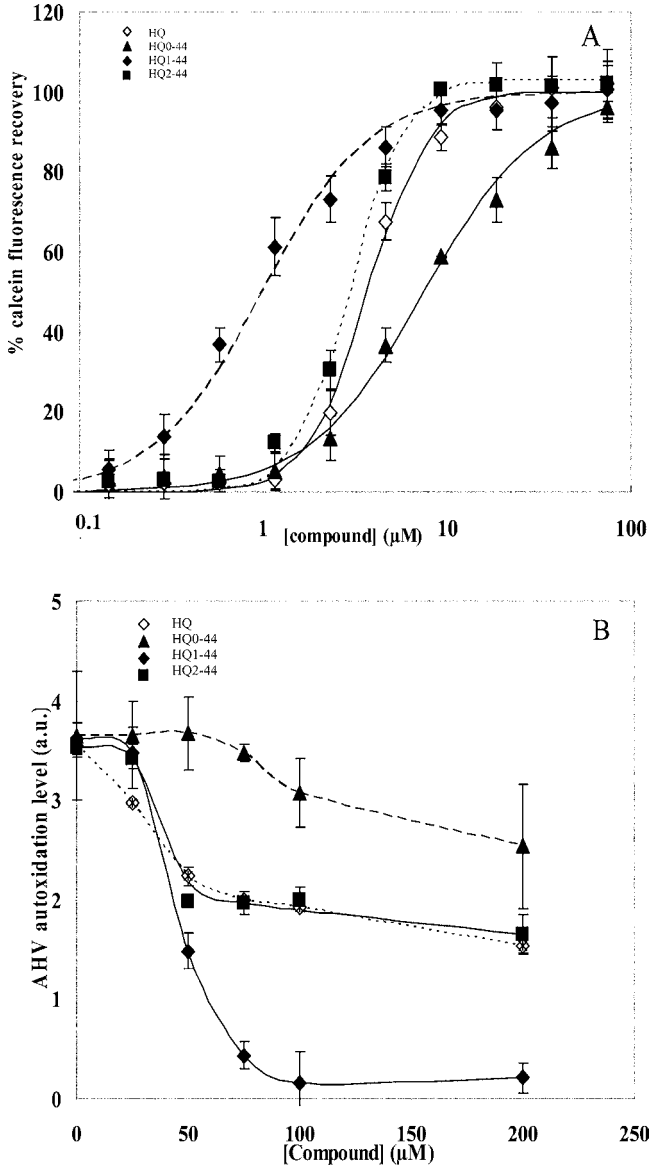

Figure 10. Comparison of the iron-chelating efficiency of Quilamines **HQ0−44**, **HQ1−44**, and **HQ2−44** with the reference chelator **HQ** in a cell-free system (A, calcein fluorescence measurements; B, HVA autoxidation test).

dx.doi.org/10.1021/bc4004734 | *Bioconjugate Chem.* 2014, 25, 320−334

HQ1−44 totally inhibited HVA autoxidation at concentrations higher than 100 μM, while only a partial decrease in this process was observed with all other compounds in this range of concentrations. The efficiency of the Quilamines to inhibit HVA autoxidation was in the following order: **HQ1−44** > **HQ2−44** = **HQ** > **HQ0−44**. These results indirectly confirmed the chelating efficiency of the various Quilamines deduced from the calcein assay. The best chelating ability of **HQ1−44** to chelate iron could explain its higher antiproliferative efficiency.

CONCLUSION

As previous data suggested that Quilamine **HQ1−44** represents an interesting tool in antineoplastic therapy, our objective was to design a second generation of Quilamines by changing the length and the nature of the spacer between 8-hydroxyquinoline and the homospermidine chain, which seems to be the polyamine most efficiently vectorized by the PTS. Starting from homospermidine **1**, three new Quilamines, **HQ2−44**, **HQCO-44**, and **HQCS-44**, were obtained via a Michael addition, peptide linkage or by using the Willgerodt-Kindler reaction. Following deprotection of the amine functions, these second-generation Quilamines were isolated in respective overall yields of 38% (9 steps), 48% (6 steps), and 30% (6 steps). After adapting the synthetic strategy, Quilamine **HQ0−44** was obtained in 7 steps with an overall yield of 23% by using polyamine functionalized by an aldehyde.

The biological evaluation of these second-generation Quilamines showed that modifying the size of the spacer increased the selectivity of these compounds for the PTS. Moreover, assessing the toxicity of Quilamines **HQ0−44** and **HQ2−44** highlighted their marked antiproliferative effect on several cancerous cell lines as well as a differential activity on nontransformed cells (fibroblasts). The HCT116 cell line, originating from a human colon adenocarcinoma, was the most responsive to the various Quilamines, while MDA-MB231 (breast cancer), PC3 (prostate cancer), NCI-H727 (lung cancer), and Hacat (human immortalized keratinocyte) tumor cell lines did not show an antiproliferative effect. In contrast, Quilamines **HQCO-44** and **HQCS-44** presented low selectivity for the PTS, probably due to a loss of electrostatic interaction. **HQ1−44** remains the Quilamine with the strongest antiproliferative effect on human tumor cell lines and a high selectivity of uptake by the PTS. As deduced from the calcein and HVA assays the higher iron chelating capacity of **HQ1−44** could explain its higher antiproliferative efficiency. A study of the mechanism of action of this promising Quilamine in the HCT116 tumor cell line is now underway and will be published shortly.

AUTHOR INFORMATION

Corresponding Authors

*Phone: 00-33-2-23233861. Fax: 00-33-2-99540137. E-mail: francois.gaboriau@univ-rennes1.fr.

*Phone: 00-33-2-51125406. Fax: 00-33-2-51125402. E-mail: david.deniaud@univ-nantes.fr.

Notes

The authors declare no competing financial interest.

ACKNOWLEDGMENTS

The authors are grateful to the Conseil Régional Pays de la Loire, to the French Ministry of Education, to the Ligue Nationale Contre le Cancer (LNCC, Ille et Vilaine/Loire Atlantique), to the Association pour la Recherche sur le Cancer (ARC), and to the Centre National de la Recherche Scientifique (CNRS) for financial support. The cell viability measurements on the different tumor cell lines were carried out by the analytical platform ImPACcell (Imagerie pour une analyse du contenu cellulaire) of the Structure Fédérative de Recherche BIOSIT in Rennes (BiogenOuest and Cancéropôle Grand Ouest network).

REFERENCES

(1) Andrews, N. C. (2000) Iron homeostasis: insights from genetics and animal models. *Nat. Rev. Genet. 1*, 208−217.

(2) Kolberg, M., Strand, K. R., Graff, P., and Andersson, K. K. (2004) Structure, function, and mechanism of ribonucleotide reductases. *Biochem. Biophys. Acta 1699*, 1−34.

(3) Strand, K. R., Karlsen, S., Kolberg, M., Rohr, A. K., Gorbitz, C. H., and Andersson, K. K. (2004) Crystal structural studies of changes in the native dinuclear iron center of ribonucleotide reductase protein R2 from mouse. *J. Biol. Chem. 279*, 46794−46801.

(4) Elford, H. L., Freese, M., Passamani, E., and Morris, H. P. (1970) Ribonucleotide reductase and cell proliferation. I. Variations of ribonucleotide reductase activity with tumor growth rate in a series of rat hepatomas. *J. Biol. Chem. 245*, 5228−5233.

(5) Merlot, A. M., Kalinowski, D. S., and Richardson, D. R. (2013) Novel chelators for cancer treatment: where are we now? *Antioxid. Redox Signal. 18*, 973−1006.

(6) Brookes, M. J., Hughes, S., Turner, F. E., Reynolds, G., Sharma, N., Ismail, T., Berx, G., McKie, A. T., Hotchin, N., Anderson, G. J., Iqbal, T., and Tselepis, C. (2006) Modulation of iron transport proteins in human colorectal carcinogenesis. *Gut 55*, 1449−1460.

(7) Boult, J., Roberts, K., Brookes, M. J., Hughes, S., Bury, J. P., Cross, S. S., Anderson, G. J., Spychal, R., Iqbal, T., and Tselepis, C. (2008) Overexpression of cellular iron import proteins is associated with malignant progression of esophageal adenocarcinoma. *Clin. Cancer Res. 14*, 379−87.

(8) Jiang, X. P., Elliott, R. L., and Head, J. F. (2010) Manipulation of iron transporter genes results in the suppression of human and mouse mammary adenocarcinomas. *Anticancer Res. 30*, 759−65.

(9) Pinnix, Z. K., Miller, L. D., Wang, W., D'Agostino, R., Jr., Kute, T., Willingham, M. C., Hatcher, H., Tesfay, L., Sui, G., Di, X., Torti, S. V., and Torti, F. M. (2010) Ferroportin and iron regulation in breast cancer progression and prognosis. *Sci. Transl. Med. 2*, 43−56.

(10) Wallace, H. M., Fraser, A. V., and Hughes, A. (2003) A perspective of polyamine metabolism. *Biochem. J. 376*, 1−14.

(11) Grillo, M. A., and Colombatto, S. (1994) Polyamine transport in cells. *Biochem. Soc. Trans. 22*, 894−898.

(12) Palmer, A. J., and Wallace, H. M. (2010) The polyamine transport system as a target for anticancer drug development. *Amino Acids 38*, 415−422.

(13) Seiler, N. (2003) Thirty years of polyamine-related approaches to cancer therapy. Retrospect and prospect. Part 2. Structural analogues and derivatives. *Curr. Drug Targets 4*, 565−585.

(14) Seiler, N. (2003) Thirty years of polyamine-related approaches to cancer therapy. Retrospect and prospect. Part 1. Selective enzyme inhibitors. *Curr. Drug Targets 4*, 537−564.

(15) Holley, J. H., Mather, A., Cullis, P., Symons, M. R., Wardman, P., Watt, R. A., and Cohen, G. M. (1992) Uptake and cytotoxicity of novel nitroimidazole-polyamine conjugates in Ehrlich ascites tumour cells. *Biochem. Pharmacol. 43*, 763−769.

(16) Verschoyle, R. D., Carthew, P., Holley, J. L., Cullis, P., and Cohen, G. M. (1994) The comparative toxicity of chlorambucil and chlorambucil-spermidine conjugate to BALB/c mice. *Cancer Lett. 85*, 217−222.

(17) Delcros, J. G., Tomasi, S., Carrington, S., Martin, B., Renault, J., Blagbrough, I. S., and Uriac, P. (2002) Effect of spermine conjugation on the cytotoxicity and cellular transport of acridine. *J. Med. Chem. 45*, 5098−5111.

(18) Phanstiel, O., IV, Kaur, N., and Delcros, J. G. (2007) Structure-activity investigations of polyamine-anthracene conjugates and their uptake via the polyamine transporter. *Amino Acids 33*, 305−313.
(19) Dallavalle, S., Giannini, G., Alloatti, D., Casati, A., Marastoni, E., Musso, L., Merlini, L., Morini, G., Penco, S., Pisano, C., Tinelli, S., De Cesare, M., Beretta, G. L., and Zunino, F. (2006) Synthesis and cytotoxic activity of polyamine analogues of camptothecin. *J. Med. Chem. 49*, 5177−5186.
(20) Esteves-Souza, A., Lucio, K. A., Da Cunha, A. S., Da Cunha Pinto, A., Da Silva Lima, E. L., Camara, C. A., Vargas, M. D., and Gattass, C. R. (2008) Antitumoral activity of new polyamine-naphthoquinone conjugates. *Oncol. Rep. 20*, 225−231.
(21) Tomasi, S., Renault, J., Martin, B., Duhieu, S., Cerec, V., Le Roch, M., Uriac, P., and Delcros, J. G. (2010) Targeting the polyamine transport system with benzazepine- and azepine-polyamine conjugates. *J. Med. Chem. 53*, 7647−7663.
(22) Burns, M. R., Graminski, G. F., Weeks, R. S., Chen, Y., and O'Brien, T. G. (2009) Lipophilic lysine-spermine conjugates are potent polyamine transport inhibitors for use in combination with a polyamine biosynthesis inhibitor. *J. Med. Chem. 52*, 1983−1993.
(23) Covassin, L., Desjardins, M., Soulet, D., Charest-Gaudreault, R., Audette, M., and Poulin, R. (2003) Xylylated dimers of putrescine and polyamines: influence of the polyamine backbone on spermidine transport inhibition. *Bioorg. Med. Chem. Lett. 13*, 3267−3271.
(24) Delcros, J. G., Vaultier, M., Le Roch, N., Havouis, R., Moulinoux, J. P., and Seiler, N. (1997) Bis(7-amino-4-azaheptyl)-dimethylsilane: a new tetramine with polyamine-like features. Effects on cell growth. *Anti Cancer Drug Des. 12*, 35−48.
(25) Martin, B., Posseme, F., Le Barbier, C., Carreaux, F., Carboni, B., Seiler, N., Moulinoux, J. P., and Delcros, J. G. (2002) (Z)-1,4-diamino-2-butene as a vector of boron, fluorine, or iodine for cancer therapy and imaging: synthesis and biological evaluation. *Bioorg. Med. Chem. 10*, 2863−2871.
(26) Zhuo, J. C., Cai, J., Soloway, A. H., Barth, R. F., Adams, D. M., Ji, W., and Tjarks, W. (1999) Synthesis and biological evaluation of boron-containing polyamines as potential agents for neutron capture therapy of brian tumors. *J. Med. Chem. 42*, 1282−1292.
(27) Wang, C., Delcros, J. G., Biggerstaff, J., and Phanstiel, O. t. (2003) Molecular requirements for targeting the polyamine transport system. Synthesis and biological evaluation of polyamine-anthracene conjugates. *J. Med. Chem. 46*, 2672−2682.
(28) Wang, C., Delcros, J. G., Biggerstaff, J., and Phanstiel, O., IV (2003) Synthesis and biological evaluation of N1-(anthracen-9-ylmethyl)triamines as molecular recognition elements for the polyamine transporter. *J. Med. Chem. 46*, 2663−2671.
(29) Annereau, J. P., Brel, V., Dumontet, C., Guminski, Y., Imbert, T., Broussas, M., Vispe, S., Breand, S., Guilbaud, N., Barret, J. M., and Bailly, C. (2010) A fluorescent biomarker of the polyamine transport system to select patients with AML for F14512 treatment. *Leuk. Res. 34*, 1383−1389.
(30) Kruczynski, A., Vandenberghe, I., Pillon, A., Pesnel, S., Goetsch, L., Barret, J. M., Guminski, Y., Le Pape, A., Imbert, T., Bailly, C., and Guilbaud, N. (2011) Preclinical activity of F14512, designed to target tumors expressing an active polyamine transport system. *Invest. New Drugs 29*, 9−21.
(31) Corce, V., Morin, E., Guiheneuf, S., Renault, E., Renaud, S., Cannie, I., Tripier, R., Lima, L. M., Julienne, K., Gouin, S. G., Loreal, O., Deniaud, D., and Gaboriau, F. (2012) Polyaminoquinoline iron chelators for vectorization of antiproliferative agents: design, synthesis, and validation. *Bioconjugate Chem. 23*, 1952−1968.
(32) Byers, T. L., and Pegg, A. E. (1989) Properties and physiological function of the polyamine transport system. *Am. J. Physiol. 257*, C545−C553.
(33) Mandel, J. L., and Flintoff, W. F. (1978) Isolation of mutant mammalian cells altered in polyamine transport. *J. Cell. Physiol. 97*, 335−343.
(34) Rodbard, D., and McClean, S. W. (1977) Automated computer analysis for enzyme-multiplied immunological techniques. *Clin. Chem. 23*, 112−115.
(35) Thomas, F., Serratrice, G., Béguin, C., Saint Aman, E., Pierre, J. L., Fontecave, M., and Laulhère, J. P. (1999) Calcein as a fluorescent probe for ferric iron. *J. Biol. Chem. 274*, 13375−13383.
(36) Gaboriau, F., Delcros, J. G., and Moulinoux, J. P. (2002) A simple assay for the measurement of plasma antioxidant status using spontaneous autoxidation of homovanillic acid. *J. Pharmacol. Toxicol. Methods 47*, 33−43.
(37) Xie, S., Cheng, P., Liu, G., Ma, Y., Zhao, J., Chehtane, M., Khaled, A. R., Phanstiel, O., IV, and Wang, C. (2007) Synthesis and bioevaluation of N-(arylalkyl)-homospermidine conjugates. *Bioorg. Med. Chem. Lett. 17*, 4471−4475.
(38) Bruice, T. C., Tsubouchi, A., Dempcy, R. O., and Olson, L. P. (1996) One- and two-metal ion catalysis of the hydrolysis of adenosine 3′-alkyl phosphate esters. Models for one- and two-metal ion catalysis of RNA hydrolysis. *J. Am. Chem. Soc. 118*, 9867−9875.
(39) Abdel-Magid, A. F., Carson, K. G., Harris, B. D., Maryanoff, C. A., and Shah, R. D. (1996) Reductive amination of aldehydes and ketones with sodium triacetoxyborohydride. studies on direct and indirect reductive amination procedures. *J. Org. Chem. 61*, 3849−3862.
(40) Yoneda, A., and Azumi, T. (1984) Synthesis of 2-vinyl-8-quinolinol and measurement of stability of its metal complexes. *Chem. Lett. 13*, 1191−1194.
(41) Backeberg, O. G., and Staskun, B. (1962) A novel reduction of nitriles to aldehydes. *J. Chem. Soc.*, 3961−3963.
(42) Robinson, A., and Aggarwal, V. K. (2010) Asymmetric total synthesis of solandelactone E: Stereocontrolled synthesis of the 2-ene-1,4-diol core through a lithiation−borylation−allylation sequence. *Angew. Chem., Int. Ed. Engl. 49*, 6673−6675.
(43) Fry, J. L., and Ott, R. A. (1981) Aldehydes from nitriles. Formation of N-alkylnitrilium ions and their reduction to N-alkylaldimines by organosilicon hydrides. *J. Org. Chem. 46*, 602−607.
(44) Kaur, N., Delcros, J.-G., Martin, B., and Phanstiel, O. (2005) Synthesis and biological evaluation of dihydromotuporamine derivatives in cells containing active polyamine transporters. *J. Med. Chem. 48*, 3832−3839.
(45) De Mico, A., Margarita, R., Parlanti, L., Vescovi, A., and Piancatelli, G. (1997) A versatile and highly selective hypervalent iodine (III)/2,2,6,6-Tetramethyl-1-piperidinyloxyl-mediated oxidation of alcohols to carbonyl compounds. *J. Org. Chem. 62*, 6974−6977.
(46) Okamoto, K., Yamamoto, T., and Kanbara, T. (2007) Efficient synthesis of thiobenzanilides by Willgerodt-Kindler reaction with base catalysts. *Synlett 2007*, 2687−2690.
(47) Chivers, T., and Drummond, I. (1972) Characterization of the trisulfur radical anion S3- in blue solutions of alkali polysulfides in hexamethylphosphoramide. *Inorg. Chem. 11*, 2525−2527.
(48) Byers, T. L., Wechter, R., Nuttall, M. E., and Pegg, A. E. (1989) Expression of a human gene for polyamine transport in Chinese-hamster ovary cells. *Biochem. J. 263*, 745−752.
(49) Gardner, R. A., Delcros, J. G., Konate, F., Breitbeil, F., Martin, B., Sigman, M., Huang, M., and Phanstiel, O., IV (2004) N1-substituent effects in the selective delivery of polyamine conjugates into cells containing active polyamine transporters. *J. Med. Chem. 47*, 6055−6069.
(50) Bergeron, R. J., Bharti, N., Wiegand, J., McManis, J. S., Yao, H., and Prokai, L. (2005) Polyamine-vectored iron chelators: the role of charge. *J. Med. Chem. 48*, 4120−4137.
(51) Bergeron, R. J., McManis, J. S., Franklin, A. M., Yao, H., and Weimar, W. R. (2003) Polyamine-iron chelator conjugate. *J. Med. Chem. 46*, 5478−5483.
(52) Lescoat, G., Léonce, S., Pierré, A., Gouffier, L., and Gaboriau, F. (2012) Antiproliferative and iron chelating efficiency of the new bis-8-hydroxyquinoline benzylamine chelator S1 in hepatocyte cultures. *Chem.-Biol. Interact. 195*, 165−172.
(53) Rodriguez-Lucena, D., Gaboriau, F., Rivault, F., Schalk, I. J., Lescoat, G., and Mislin, G. L. A. (2010) Synthesis and biological properties of iron chelators based on a bis-2-(2-hydroxy-phenyl)-thiazole-4-carboxamide or -thiocarboxamide (BHPTC) scaffold. *Bioorg. Med. Chem. 18*, 689−695.

(54) Løvaas, E. (1997) Antioxidative and metal-chelating effects of polyamines, in *Antioxidants in disease mechanisms and therapy*. (Sies, H., Ed.) pp 116−149, Academic Press.
(55) Gaboriau, F., Vaultier, M., Moulinoux, J. P., and Delcros, J. G. (2005) Antioxidative properties of natural polyamines and dimethylsilane analogues. *Redox Rep. 10*, 9−18.
(56) Palmer, B. N., and Powell, H. K. J. (1974) Polyamine complexes with seven-membered chelate rings: Complexe formation of 3-azaheptane-1,7-diamine, 4-azaoctane-1,8-diamine (spermidine), and 4,9-diazadodecane-1,12-diamine (spermine) with copper(II) and hydrogen ions in aqueous solution. *J. Chem. Soc. Dalton Trans.*, 2089−2092.